UNCLASSIFIED

AD NUMBER

AD361769

CLASSIFICATION CHANGES

TO: unclassified

FROM: secret

LIMITATION CHANGES

TO:

Approved for public release, distribution unlimited

FROM:

Distribution: DoD only: others to Director, Defense Nuclear Agency, Attn: STTI. Washington, DC 20305.

AUTHORITY

DNA ltr. 31 Mar 94; DNA ltr. 31 Mar 94

THIS PAGE IS UNCLASSIFIED

No. of 190 Copies, Series

Operation
REDWING

PACIFIC PROVING GROUNDS

May - July 1956

Project 1.2

BLAST MEASUREMENTS on a
MEDIUM-YIELD SURFACE BURST(U)

Issuance Date: January 7, 1960

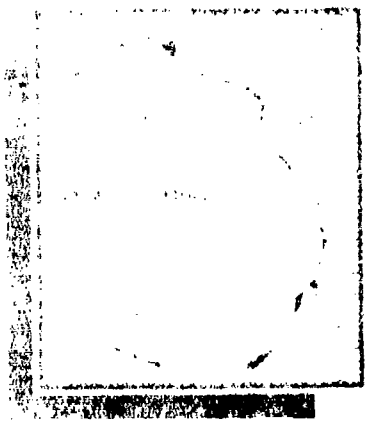

FORMERLY RESTRICTED DATA

Handle as Restricted Data in foreign dissemination. Section 144b, Atomic Energy Act of 1954.

This material contains information affecting the national defense of the United States within the meaning of the espionage laws, Title 18, U.S.C., Secs. 793 and 794, the transmission or revelation of which in any manner to an unauthorized person is prohibited by law.

HEADQUARTERS FIELD COMMAND, DEFENSE ATOMIC SUPPORT AGENCY
SANDIA BASE, ALBUQUERQUE, NEW MEXICO

SECRE

Inquiries relative to this report may be made to

Chief, Defense Atomic Support Agency
Washington 25, D. C.

When no longer required, this document may be destroyed in accordance with applicable security regulations.

DO NOT RETURN THIS DOCUMENT

ASTIA Technical Information Service Agency
Oak Ridge, Tennessee

SECRET

WT—1302

OPERATION REDWING—PROJECT 1.2

BLAST MEASUREMENTS on a MEDIUM—YIELD SURFACE BURST (U)

C.D. Broyles

Sandia Corporation
Albuquerque, New Mexico

U. S. MILITARY AGENCIES [illegible] OF THIS REPORT DIRECTLY FROM DDC. OTHER [illegible] THROUGH Sponsoring Agency to:
Director
Defense Atomic Support Agency
Washington, D. C. 20301

FORMERLY RESTRICTED DATA

Handle as Restricted Data in foreign dissemination. Section 144b, Atomic Energy Act of 1954.

This material contains information affecting the national defense of the United States within the meaning of the espionage laws, Title 18, U.S.C., Secs. 793 and 794, the transmission or revelation of which in any manner to an unauthorized person is prohibited by law.

DDC
JUN [illegible]

SECRET

GA [illegible]
Excluded from automatic downgrading and declassification

ABSTRACT

Overpressure and dynamic pressure were measured as a function of time and distance (690 to 3,250 feet) on a surface burst of a medium yield (40 kt) nuclear device on Site Yvonne, Eniwetok. Overpressures were measured with ground baffles and pitot-static gages. A precursor formed but died out at an unusually high overpressure of between 35 and 55 psi. The usual high dynamic pressures associated with precursors were observed. Outside of the limited region in which the precursor existed, the overpressure and dynamic pressure measurements were in agreement with previous measurements on surface bursts. They were consistent with the free-air values for 1.6 times the actual yield of 39.5 kt.

FOREWORD

This report presents the final results of one of the projects participating in the military-effect programs of Operation Redwing. Overall information about this and the other military-effect projects can be obtained from WT-1344, the "Summary Report of the Commander, Task Unit 3." This technical summary includes: (1) tables listing each detonation with its yield, type, environment, meteorological conditions, etc.; (2) maps showing shot locations; (3) discussions of results by programs; (4) summaries of objectives, procedures, results, etc., for all projects; and (5) a listing of project reports for the military-effect programs.

CONTENTS

ABSTRACT ---- 4

FOREWORD ---- 4

CHAPTER 1 OBJECTIVE AND BACKGROUND ---- 7
1.1 Objective ---- 7
1.2 Background ---- 7
1.3 Precursor Prediction ---- 11

CHAPTER 2 EXPERIMENT DESIGN ---- 15
2.1 Instrumentation and Recording System ---- 15
2.2 Gage Layout ---- 15

CHAPTER 3 RESULTS ---- 18
3.1 Arrival Times ---- 18
3.2 Overpressures ---- 18
3.3 Dynamic Pressures ---- 20
3.4 Impulses ---- 20
3.5 Durations ---- 36
3.6 General ---- 36

CHAPTER 4 CONCLUSIONS AND RECOMMENDATIONS ---- 37
4.1 Conclusions ---- 37
4.2 Recommendations ---- 37

REFERENCES ---- 38

APPENDIX THERMAL FLUX FROM A SURFACE BURST ---- 40

FIGURES
1.1 Precursor chart ---- 8
1.2 Precursor velocity versus normal component of thermal radiation ---- 10
1.3 Thermal radiation versus shock arrival time ---- 12
1.4 Thermal versus total yield ---- 13
2.1 Gage layout ---- 15
2.2 Details of gage stations ---- 16
3.1 Arrival time versus ground range ---- 23
3.2 Overpressure versus ground range ---- 24
3.3 Dynamic pressure versus ground range ---- 25
3.4 Impulse versus ground range ---- 26
3.5 Duration versus ground range ---- 27
3.6 Overpressure versus time, showing shock-wave arrival time, in seconds, and history after shock arrival ---- 28
3.7 Smoothed overpressure versus time records ---- 30
3.8 Overpressure versus time, showing shock-wave arrival time, in seconds, and history after shock arrival ---- 32
3.9 Dynamic pressure versus time records ---- 34

3.10 Smoothed dynamic pressure versus time records ---------- 35
A.1 Hemispherical diffusing surface and equivalent disc ---------- 41
A.2 Component of radiation normal to surface from a hemispherical source ---------- 41
A.3 Greenhouse Dog thermal radiation versus ground distance ---------- 42

TABLES

2.1 Shot Lacrosse Instrumentation and Pressure Predictions ---------- 17
3.1 Overpressure Results ---------- 19
3.2 Dynamic Pressure Results ---------- 20
3.3 Overpressure Results Scaled to 1 kt, Sea Level ---------- 21
3.4 Dynamic Pressure Results Scaled to 1 kt, Sea Level ---------- 22
3.5 Scaling Factors and Ambient Conditions for Shot Lacrosse ---------- 22
A.1 Greenhouse Dog Preshock Thermal Radiation ---------- 43

Chapter 1
OBJECTIVE and BACKGROUND

1.1 OBJECTIVE

The objective of this project was the measurement of overpressure and dynamic pressure as a function of time and distance from a surface burst of a medium-yield atomic device, a yield range not previously examined experimentally for this type burst.

1.2 BACKGROUND

Surface bursts on which overpressure (References 1,2, and 3) and dynamic pressure (References 4 and 5) have been measured represent extremes. The Jangle surface shot was a 1-kt burst with the shock wave propagated over land, and the shots during Ivy and Castle were megaton-range detonations with the shock wave traveling mainly over water.

For all the large-yield shots, yields were determined from early fireball radii versus time measurements with the assumption that the hemispherical fireball corresponds to a free-air burst of twice the actual energy release (2W theory). Pressure measurements gave pressure versus distance data that scaled as the cube root of the yield but that corresponded to approximately 1.6 instead of 2 times (Reference 3) the fireball yields. Some small distortions of the initial portion of pressure waves have been measured, but in general the shock waves are approximately ideal. The distortions and small anomalies in the dynamic pressure have been attributed to a mechanical interaction of the shock with the rough water surface and the loading of the air with water spray (References 3 and 6). These distortions have generally not resembled precursors as observed on low air bursts in Nevada. However, on Castle Shot 6 at about the 43-psi level the rounding of the shock pressure-time record was reminiscent of the precursor records near the point where the precursor dies out.

The two methods of predicting precursors (References 7 and 8), Figure 1.1, predict that a precursor will not form for a 40-kt surface burst or for one of any yield although the band of uncertainty given by Shelton would allow a precursor for yields greater than about 100 kt. Both methods presume that the precursor is caused by the formation of a surface layer of air heated by the thermal radiation from the burst. This radiation heats a surface layer of air which refracts the shock wave causing it to run ahead of the main shock, thus the name precursor.

The Armed Forces Special Weapons Project-Naval Ordnance Laboratory (AFSWP-NOL) scheme has three criteria (Reference 8):

1. Sufficient thermal radiation arrives to heat about a 5-foot layer of air and this condition is satisfied if the true height of burst is such that $(W/h^2) \geq 5$, where W is the yield in kilotons and h is the height of burst in thousands of feet.

2. The scaled height of burst $(h/W^{1/3})$ is large enough so that the cosine law does not reduce the normal component of the thermal radiation too drastically. This is assumed satisfied if $(h/W^{1/3}) \geq 50$.

3. The time before shock arrival is short enough so that the heated layer does not dissipate. This is assumed satisfied if the arrival time at ground zero is less than 0.5 second.

These criteria are logical, but the assumptions about the conditions under which they are satisfied are admittedly highly arbitrary.

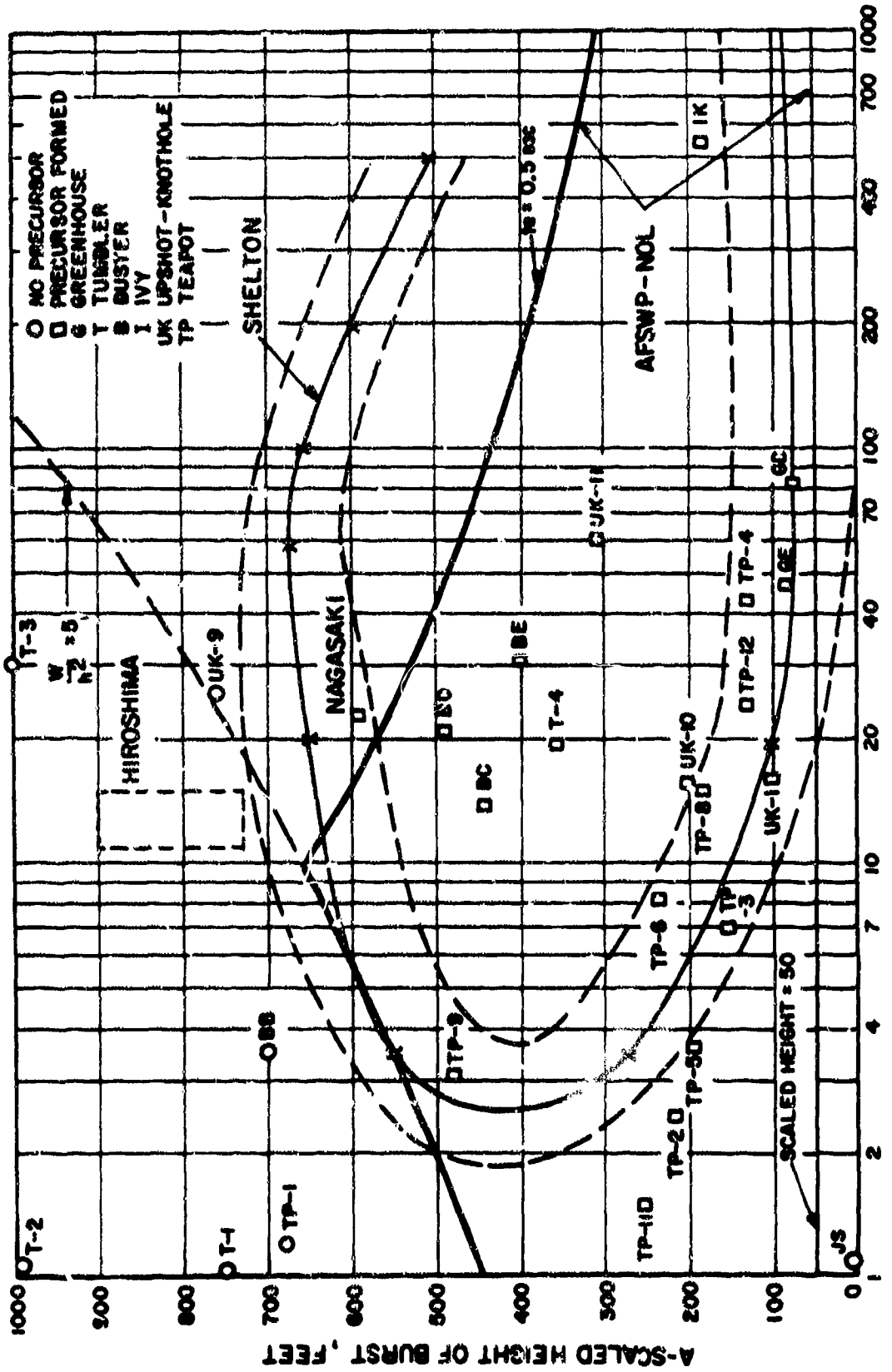

Figure 1.1 Precursor chart.

Shelton (Reference 7) applies empirical data to evaluate some constants that appear in the theoretical analysis of the refraction of a sound wave in a thermal layer. His basic criterion is that the sound speed, C', in the heated layer is high enough so that the refracted shock front becomes normal to the surface and then begins to travel faster than the intersection of the incident shock with the ground. For ambient sound speed, C, and the angle α, that the incident shock front makes with the ground, this will occur when

$$C' = C/\sin\alpha \quad \text{(Snells' Law)} \tag{1.1}$$

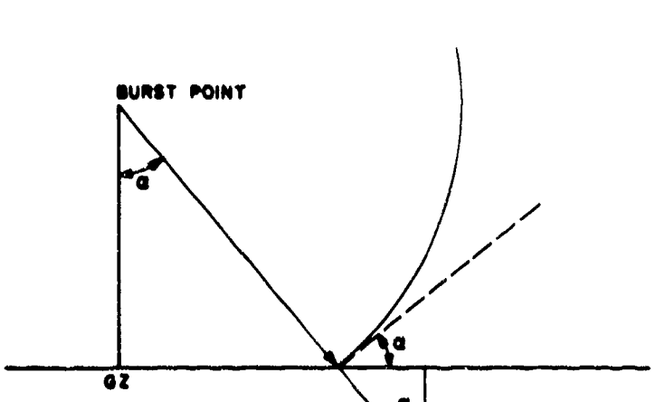

From data on one shot (Tumbler 4) Shelton used the measured precursor velocities, pressures, arrival times, the Rankine-Hugoniot relations, and the calculated components of thermal radiation incident normal to the surface before shock arrival ($Q_{\perp ps}$) to obtain a relation between the sound velocity in the heated layer and $Q_{\perp ps}$. For preparing his precursor prediction chart, the known thermal radiation pulse shape, the height of burst, and the above relation were used. $Q_{\perp ps}$ was calculated by assuming a point source and taking the cosine of the angle of incidence to obtain the normal component. To extend his curves to yields over 30 kt, Shelton assumed that the fraction of the energy emitted at times scaled as $W^{1/3}$ would vary as $W^{-1/6}$ since thermal times are proportional to $W^{1/2}$. This extension does not appear proper since it seems to imply a linear relation between thermal radiation versus time.

Shelton (Reference 8, page 40) has also pointed out other factors involved, such as the finite size of the fireball, its rate of rise, and the fact that with increasing yield, low bursts will have smaller and smaller fractions of their surfaces obscured by dust.

In addition to the time delay because of the rate of emission of the thermal radiation, a finite time is required to heat the air. Two mechanisms have been postulated for this heating, and both probably contribute to it. The so-called popcorn effect, in which water of hydration causes the grains to explode, is a rapid method of heating the air; however, turbulent convection and expansion can also take place rapidly enough (Reference 9) to provide a heated layer before shock arrival.

The ideas and methods outlined above are of great value, but since they are semi empirical and somewhat arbitrary in their choice of parameters, there is a need to extend them.

During Operation Teapot a comparison of the two methods was made, and it was concluded that the existence of precursors on Shots 2, 5, and 11, where Shelton had predicted none, favored the AFSWP-NOL method (Reference 10). The evidence could just as easily, in fact more reasonably, be interpreted to mean that Shelton's curve should be modified. Shots 2 and 5 showed the typical precursor hump in the pressure-distance curve, and the pressure-time records showed the typical development and decay of the precursor with ground distance. However, Shot 11, which was farthest from Shelton's curve (Figure 1.1), showed only one dynamic pressure record

that departed markedly from ideal, and there was almost no evidence of the hump in the pressure-distance curve. This would indicate that Shot 11 was on the edge of the precursor region and that Shelton's constants should be modified to put his curve through this point.

There are other indications that his curve should be modified. First, his use of the Rankine-Hugoniot relations to obtain sound speed from the precursor speed can be questioned since the precursor is a slow rising pressure wave and therefore should be traveling with sonic velocity. The appropriate modification would make the thermal radiation more effective in the empirical correlation of thermal radiation with sound speed and would move Shelton's curve in the correct direction to be compatible with the Operation Teapot results. Figure 1.2 suggests another modification to his procedure; that is, some sort of height of burst and yield dependence is needed

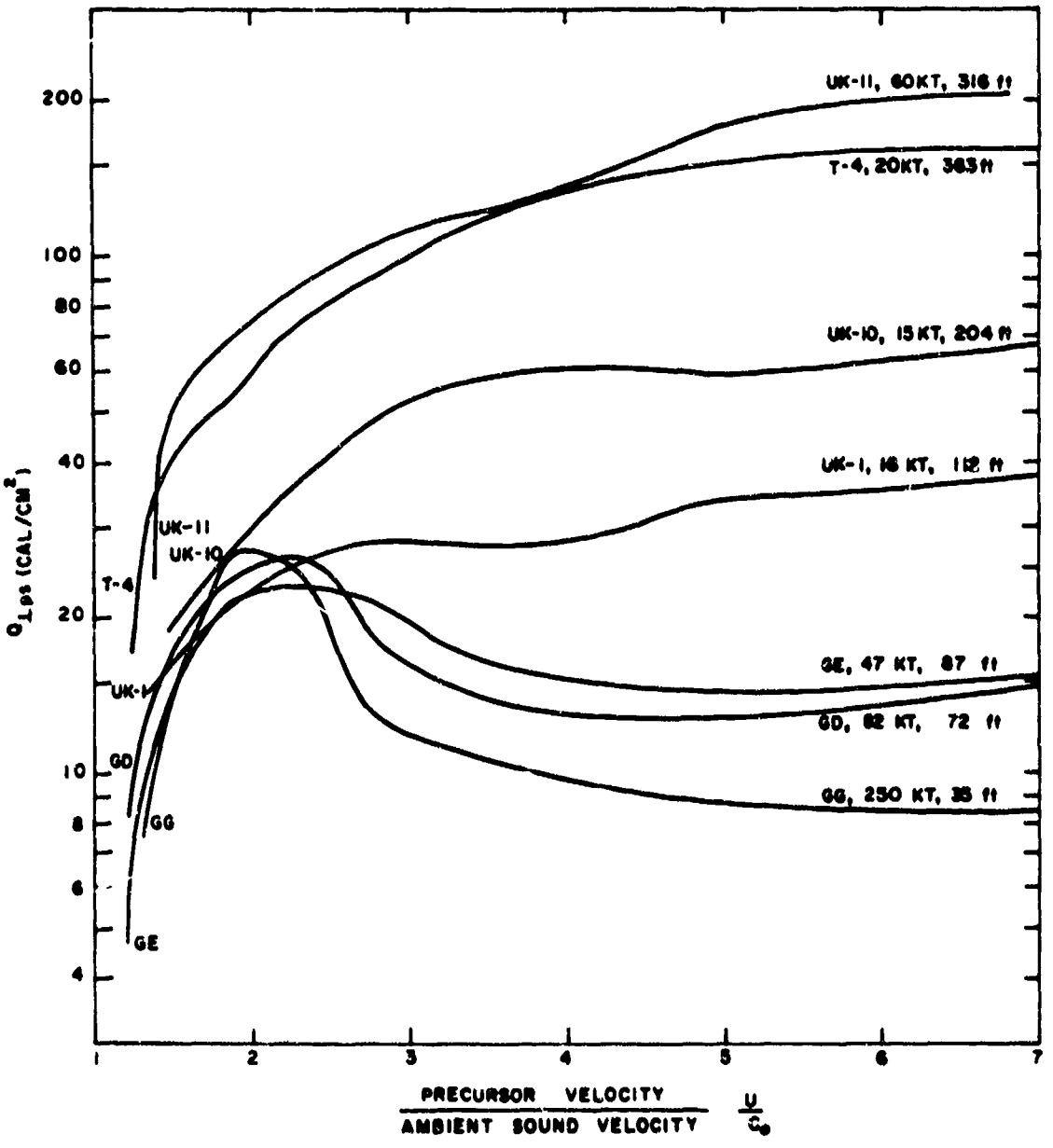

Figure 1.2 Precursor velocity versus normal component of thermal radiation.

for the relationship between the sound velocity in the heated layer and the amount of preshock thermal radiation since as is evident the relationship does vary for both height of burst and yield.

In opposition to the AFSWP-NOL assumption of no precursor below a scaled height of burst of 50 feet, photographs of Trinity and Greenhouse George, both at scaled heights of approximately

35 feet, show evidence of some sort of disturbance running ahead of the main shock and Mach stem. Unfortunately, no pressure-time records were obtained on either shot so the extent or effect of the disturbances cannot be evaluated.

1.3 PRECURSOR PREDICTION

Without trying to draw a new quantitative prediction chart at this time, previous shots and some calculations for surface bursts to obtain a better understanding of the possibilities of precursor formation from surface bursts can be examined.

Use is made of two qualitative concepts: (1) the larger the product $Q_{\perp ps}\sin\alpha$, the more probable is a precursor, and (2) if the shock arrival time, t_a, is larger than twice the time of thermal maximum, t_m, then the larger the ratio t_a/t_m, the less likely is the precursor formation.

The first criterion corresponds to that of Shelton; $Q_{\perp ps}$ is one factor that determines the temperature and therefore the sound speed in the thermal layer and sin α accounts for the inclination of the shock to the ground. The second is a generalization of the AFSWP-NOL idea that the thermal layer will dissipate if the shock does not arrive at ground zero before 0.5 second. Robertson (Reference 11) at the National Bureau of Standards has shown that for bomb-like thermal pulses the time at which the surface reaches its maximum temperature varies from 1.2 to 2.4 times the time to thermal radiation maximum. Sauer (Reference 9) has shown that for convective heat transfer, the air temperature reaches its maximum some time later than the surface. For example, with reasonable assumptions about the thermal eddy diffusivity of air, Sauer's calculations show that at 1 foot above ground the peak air temperature is reached at about twice the time to maximum surface temperature.

Plots of $Q_{\perp ps}\sin\alpha$ versus t_a/t_m for several shots are shown in Figure 1.3. The higher air burst curves have been calculated with the burst treated as a point source. The surface bursts have been treated in a way that takes account of the finite size of the fireball. The latter calculations are described in detail in the Appendix. The low air bursts are treated by a combination of the two methods, since they may be treated as surface bursts for most of the time of interest because their fireballs become hemispherical before much of the thermal radiation is emitted. The measured thermal yields, as well as arrival times, have been used for all the actual shots. The amount of thermal radiation before shock arrival has been obtained using the measured thermal versus time curve for the Upshot-Knothole and Tumbler-Snapper shots, while for the other shots the curve for Upshot-Knothole 11 was scaled as the square root of the yield. No attenuation was included in any of the calculations, and only on Castle 6 would it appreciably affect the values. Here the change did not appear significant.

Even though Upshot-Knothole 9 had $Q_{\perp ps}\sin\alpha$ values as high as some of the precursor shots (Figure 1.3), the earliest shock arrival was almost 6 times the thermal maximum time. Even so, Upshot-Knothole 9 had a well developed thermal Mach stem that even toed out slightly (References 12 and 13). Thus, Upshot-Knothole 9 seemed to be near the edge of the precursor region and served to give some idea of how late the shock arrival must be to adversely affect precursor formation. The Upshot-Knothole and Tumbler-Snapper shots that had well formed precursors were the ones with the highest peak values of the $Q_{\perp ps}$. The Jangle surface shot, on the other hand, had by far the lowest value of preshock thermal, which is consistent with the observed lack of a precursor. The Greenhouse shots were grouped with Castle 6 and the calculated 40-kt surface burst. Since Greenhouse Easy and Greenhouse Dog had precursors, one is tempted to say that Castle 6 and the 40-kt surface burst should also. Although Castle 6 did not seem to have one, there was some indication of thermal effect as mentioned in Section 1.2. Transmission measurements in approximately the same direction as the blast measurements gave a transmission of about 87 percent at the 43-psi station mentioned. This absorption, coupled with the fact that the ground was wet from rain the morning of the shot, could explain why no precursor was formed.

Two opposing factors about the 40-kt surface burst calculation are to be noted. First, the

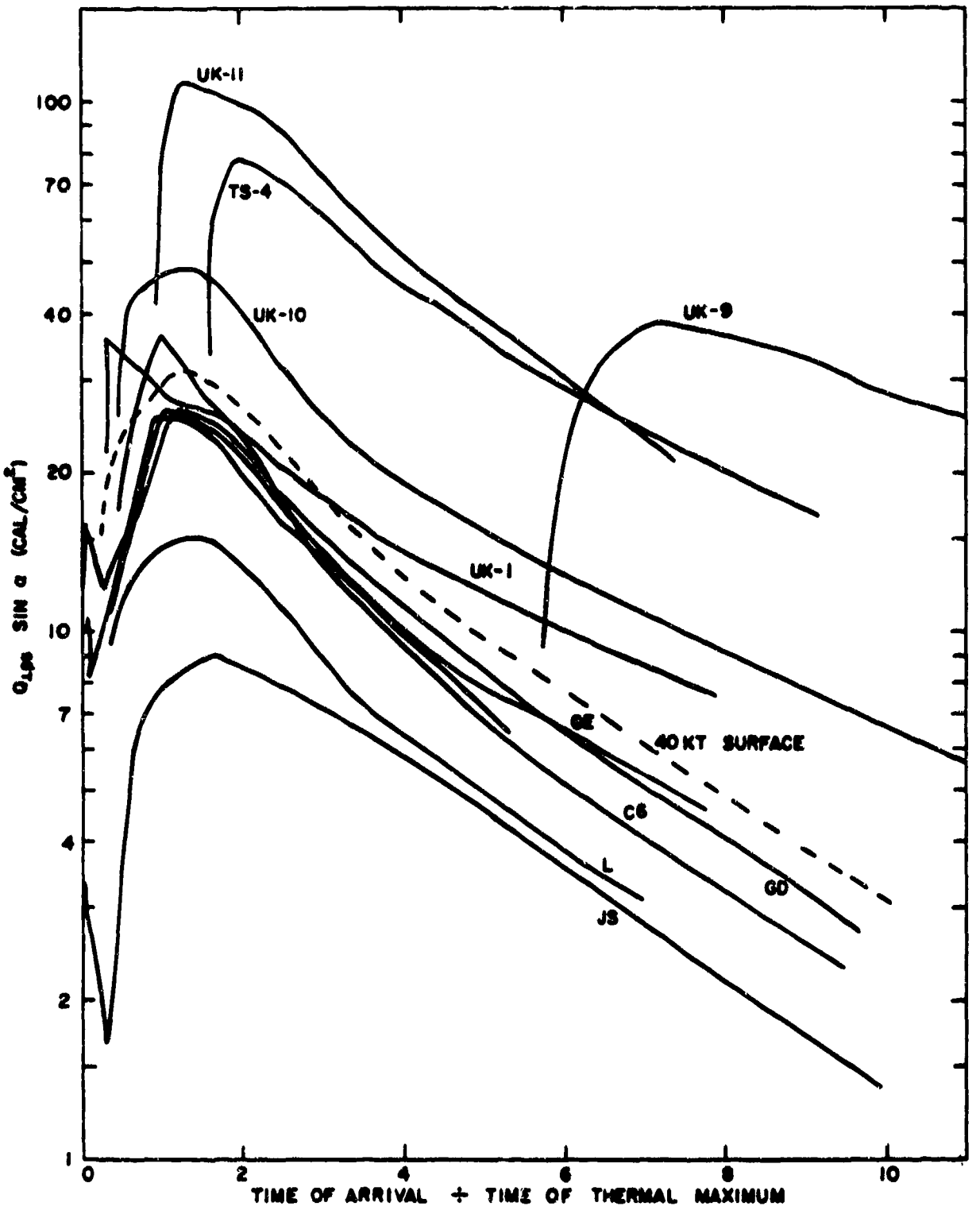

Figure 1.3 Thermal radiation versus shock arrival time.

SECRET

arrival times were taken from a 2W free-air curve, while a precursor actually formed, these times would be shorter. This would, of course, lower the amount of thermal before shock arrival. On the other hand, the thermal yield used, 10 kt, was based on Operation Greenhouse measurements, which were much lower than later and presumably more accurate measurements. If only the later measurements were considered the thermal yield would be expected to be about 15 kt. This would not change the relative likelihood of precursor formation between the 40-kt surface burst and the Greenhouse shots, but it would bring them up nearer the Nevada shots and above Castle 6 which had little sign of a precursor. The curve marked L is for Shot Lacrosse, using measured thermal yield, and will be discussed in Chapter 3.

Figure 1.4 shows that the early measurements of thermal yield made by Naval Research Laboratory (NRL) were generally lower than later ones made by either NRL or others. It should be noted that if only the later measurements (After Tumbler-Snapper) are considered, there is no apparent difference in thermal yield of high or low air bursts. Although the lower limit cov-

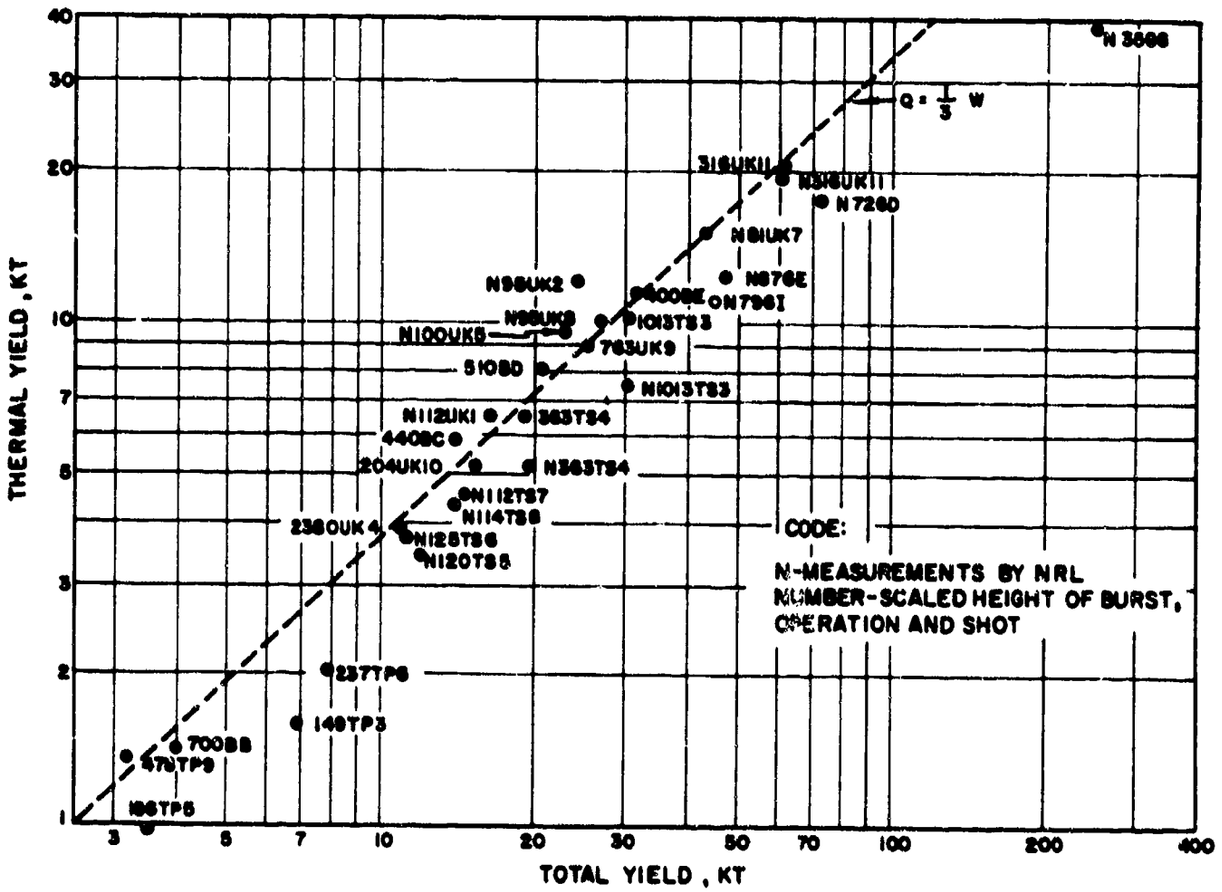

Figure 1.4 Thermal versus total yield.

ered by these measurements is about 100 feet scaled height of burst, this indicates that surface bursts should not differ either, since they are similar in shape (hemispherical) to the low air bursts during the radiation of almost all the latter's thermal energy. This means that one should not expect any appreciable reduction in thermal for surface bursts compared to air bursts as long as the yield is in the range covered by the observations, i.e., above about 10 kt. The large reduction in the thermal yield (one third of an air burst) for the Jangle surface shot, if true, must rapidly become less when the yield increases to 10 kt.

It was evident from the above reasoning that blast measurements on Shot Lacrosse could provide useful information about precursor formation. The calculations presented above show that

under certain conditions a precursor should be expected for a surface burst. Shot Lacrosse was expected to answer the question for a particular condition. Not only was the yield to be one of tactical significance, but the weather and surface conditions would be less favorable than at Nevada, since in the Pacific in May the ground could be expected to be wet and certainly the air attenuation would be higher. Thus, the results from this test would be subject to the same interpretation as previous EPG data. If a precursor formed, one might expect a more severe one in Nevada, and even if none formed, a precursor might still form in Nevada.

Chapter 2
EXPERIMENT DESIGN

2.1 INSTRUMENTATION AND RECORDING SYSTEM

Overpressures were measured with Wianko variable reluctance pressure transducers mounted in ground baffles (Reference 15) and in pitot-static gages (Reference 5). Dynamic pressures were measured with similar transducers in the pitot-static gage. The pitot-static gage mounts were of the type used in Operation Teapot (Reference 16). Information was recorded as a frequency mod-

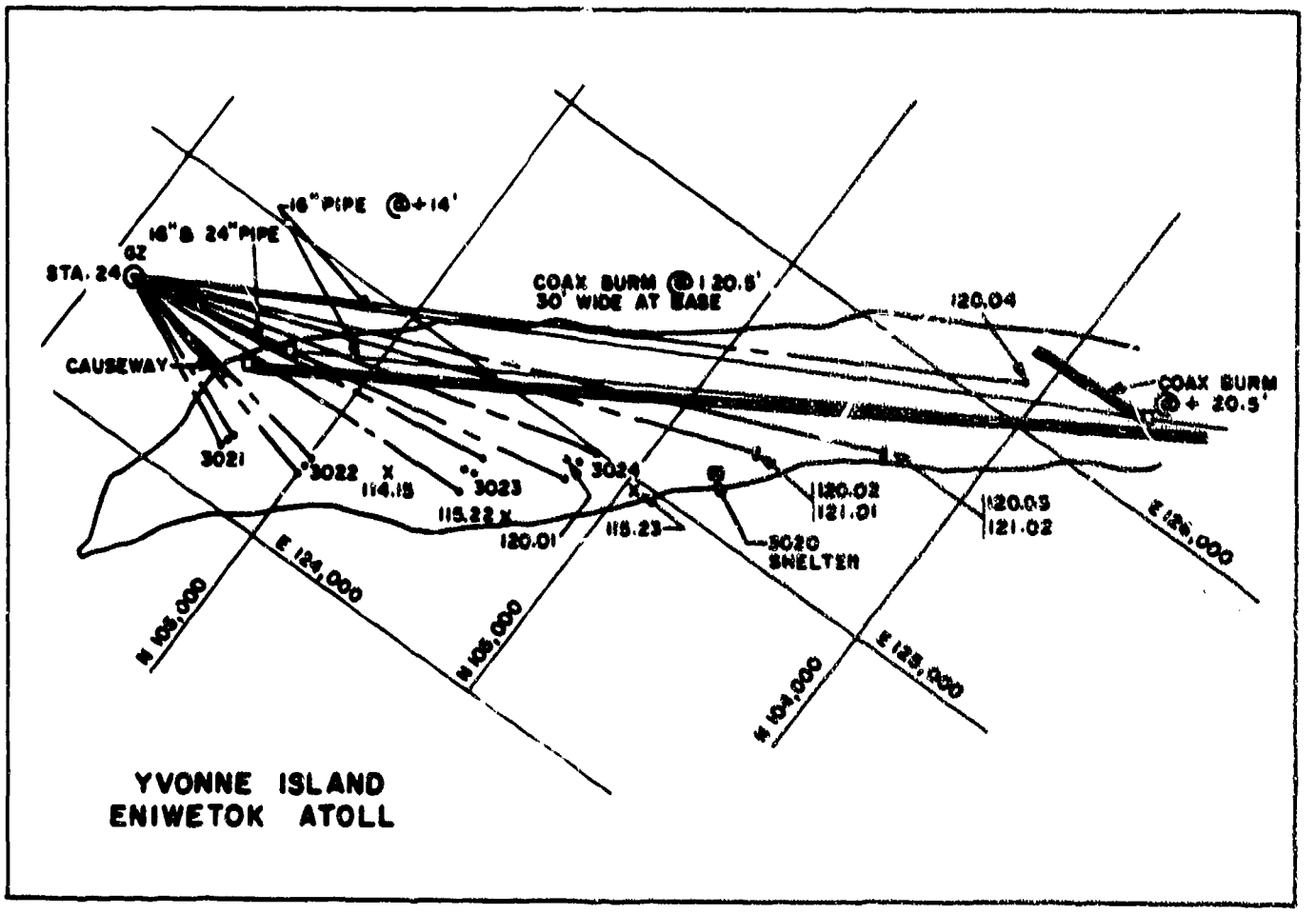

Figure 2.1 Gage layout.

ulated signal on magnetic tape. Though not identical with such systems used by Sandia Corporation in the past, use was made of Consolidated Type D System amplifiers and Ampex Model S-3439 magnetic tape transports as had previous Sandia Corporation systems (Reference 15).

2.2 GAGE LAYOUT

Layout of the blast line was made in conjunction with another of Sandia Corporation responsibilities, Project 30.2. The layout for both projects is shown in Figures 2.1 and 2.2. Project 30.2 included overpressure and dynamic pressure gages at its stations; these results will be

SECRET

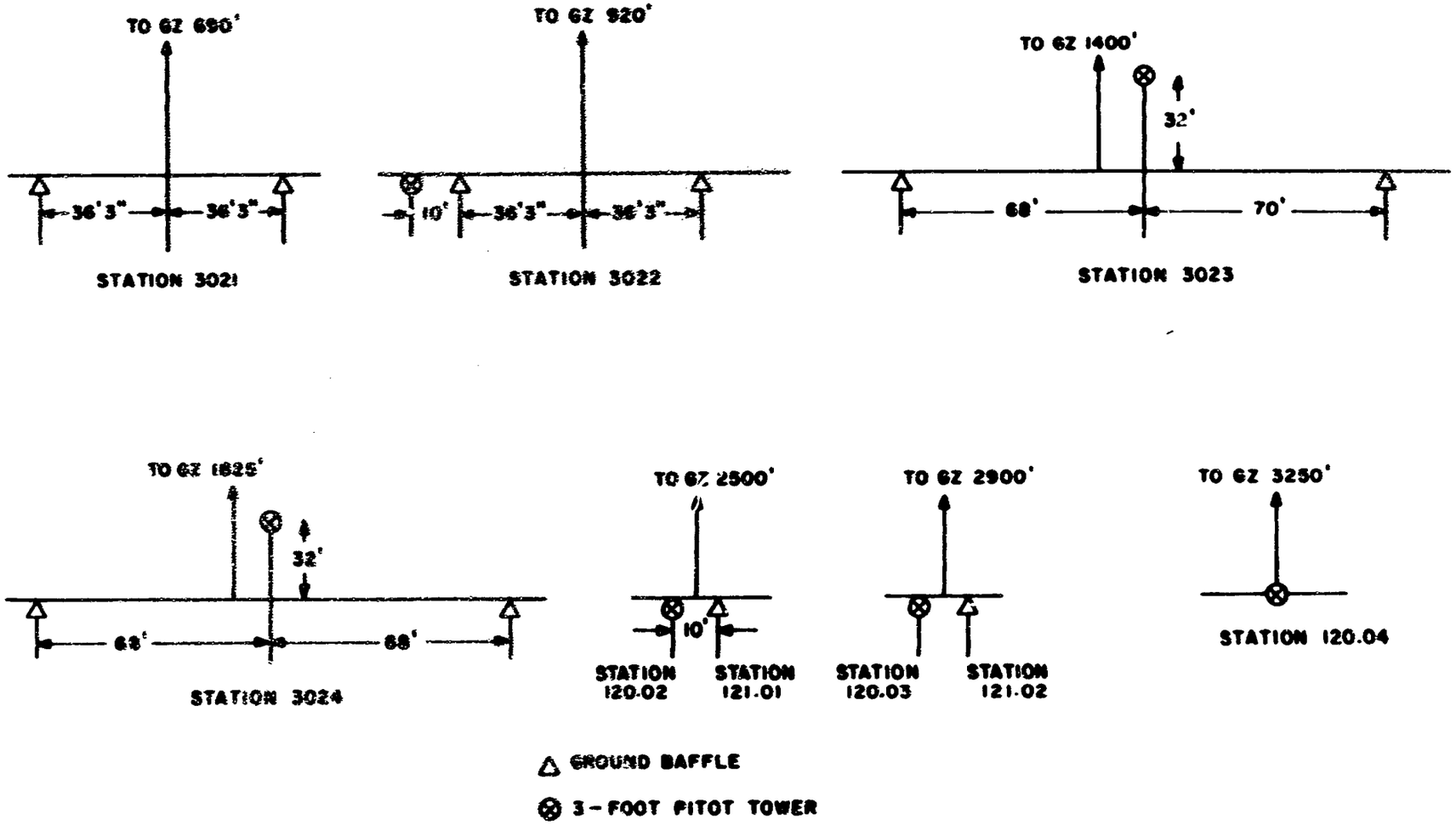

Figure 2.2 Details of gage stations.

included in the present report. Table 2.1 lists the pertinent gages, locations, and predicted blast parameters. Two sets of predictions are shown, the first based on 1.6 times the free-air values for 40 kt and the second on 2 times the free-air values. Operation Castle experience indicated the lower values would be the expected ones. However, the larger 2W values were used for set ranges, since with the yield uncertainty this provided the best protection against the signals being either so large or so small that accuracy would be lost.

The gage numbering system includes the last part of the station number, an abbreviation for the type of gage, and the height above ground if the gage is not at ground level. GB is ground

TABLE 2.1 SHOT LACROSSE INSTRUMENTATION AND PRESSURE PREDICTIONS

Station	Gage	Height	Ground Range	Overpressure		Dynamic Pressure		Arrival Time	
				1.6W	2W	1.6W	2W	1.6W	2W
		ft	ft	psi		psi		sec	
120.01	001q3,001P3	3	1,792	38	40	23	28	0.437	0.416
120.02	002q3,002P3	3	2,500	17.0	19.5	6.1	7.8	0.850	0.800
121.01	101GB	0	2,500	17.0	19.5	6.1	7.8	0.850	0.800
120.03	003q3,003P3	3	2,900	12.7	14.5	3.5	4.5	1.107	1.050
121.02	102GB	0	2,900	12.7	14.5	3.5	4.5	1.107	1.050
120.04	004q3,004P3	3	3,250	10.5	11.7	2.5	3.0	1.345	1.281
3021	1GBL,1GBR, 1GBR-RF	0	690	360	470	840	1100	0.054	0.049
3022	2GBL,2GBR	0	920	178	210	295	370	0.106	0.094
—	2q3	3	—	—	—	—	—	—	—
3023	3P3,3q3	3	1,368	64	76	63	80	0.254	0.226
—	3GBL,3GBR	0	1,400	60	72	56	75	0.267	0.244
3024	4GBL,4GBR	0	1,825	33	39	20	27	0.462	0.432

baffle, P is overpressure in the pitot gage, and q is the dynamic pressure element in the pitot gage. R and L are used on the ground baffles to indicate gages to the right or left, respectively, as one faces ground zero. Gage 1GBR-RF was recorded by wireless telemetry to Site Elmer. As an example of the numbering systems gage, 001q3 is the dynamic pressure element of a pitot-static gage at Station 120.01, mounted 3 feet above the surface of the ground.

Chapter 3
RESULTS

Results are given in Tables 3.1 and 3.2 and the results scaled to sea level and 1 kt are given in Tables 3.3 and 3.4. Pressure-time records are shown in Figures 3.6 through 3.10. The data plotted versus ground range are given in Figures 3.1 through 3.5. The pressure-time records shown in Figures 3.7 and 3.10 are smoothed records in which, by intercomparison of all records the noise and zero shifts have been extracted. Gage ringing and perhaps some small pressure fluctuations have also been smoothed through. The results in Tables 3.1 and 3.2 are derived from these smoothed curves. Scaling factors and ambient conditions for Shot Lacrosse are shown in Table 3.5.

3.1 ARRIVAL TIMES

Arrival times were consistent with 1.6 times the free-air values for the yield of 39.5 kt, and except for Station 3023 did not show the abnormally early arrival times associated with precursors. The arrival times versus ground range are plotted in Figure 3.1 along with the curves for 1.6 and 2 times the free-air values for 39.5 kt.

3.2 OVERPRESSURES

Figure 3.2 shows a comparison of the measured overpressures with the free-air pressure distance curve for 1.6 times the yield of 39.5 kt, the Naval Ordnance Laboratory pressure-distance curve measured along the surface over water, and the pressure-distance curve for an average surface taken from Capabilities of Atomic Weapons. No corrections were made to the overpressure measurements for the instruments observing precursors. Overpressures for the other gages were corrected for Mach number effects according to wind tunnel calibrations. The NOL curve and the free-air curve for 1.6 times the yield are essentially identical and the gage measurements fit these curves well within the experimental error of 5 percent with two exceptions. At 920 feet 2 GBR (Figure 3.6) shows evidence of the initiation of a precursor and the pressure is 15 percent lower than 2GBL at the same distance. At 1,400 feet both 3GBR and 3GBL (Figure 3.6) show definite precursor wave forms although the peak pressures are not reduced, as is usually the case. In fact, at this station the pitot gage, 3P3, shows an unusually high peak pressure even though having the distorted precursor wave form. The localized variation in the precursor is pointed up by the differences in the wave forms of the records obtained by the three gages at this station. The two ground baffles are at the same radial distance but are separated laterally by 138 feet. The right ground baffle, 3GBR, has a decidedly rounded main peak but does not have the front porch apparent at 3 GBL and 3P3. This is consistent with the arrival times since 3 GBL and 3P3 have the same precursor arrival times showing that the precursor front here was asymmetric, being inclined at about 25 degrees from radially outward. The pressure in the main peak, however, arrives at the two ground baffles at the same time indicating the main wave is symmetric with radius from ground zero.

Examination of Figure 2.1 shows that not only do the stations vary in ground range but also in their azimuth from ground zero. Thus, the evidence from the wave forms discussed above, that is, (1) no pressure at 2GBL (2) slight pressure at 2 GBR (3) most pronounced at 3GBL (4) less pronounced at 3GBR than 3GBL (5) none at 4GBL or 4GBR indicate that the precursor was limited in extent both in ground range and in lateral extent. The measurements made by Ballistic Research Laboratories (BRL) on this shot (Reference 16) support the limited extent of the precursor. Three of their stations, 114.15, 115.22, and 115.23 are shown in Figure 2.1.

TABLE 3.1 OVERPRESSURE RESULTS

Station	Ground Range	Gage	Arrival Time	Peak Positive Pressure	Peak Negative Pressure	Positive Pressure Duration	Negative Pressure Duration	Positive Pressure Impulse	Negative Pressure Impulse
	ft		sec	psi	psi	sec	sec	psi-sec	psi-sec
3021	690	1GBL	0.050	440		Record bad after 0.058 sec			
3021	690	1GBR	0.050	370		Record bad after 0.054 sec			
3021	690	1GBR-RF	0.050	330		Record bad after 0.090 sec			
3022	920	2GBL	0.104	155	¶	0.48	¶	11.6	¶
3022	920	2GBR	0.102	132*		Record bad after 0.113 sec			
3023	1,368	3P3	0.264	84†	4.3	0.43	4.5	4.8	7.7
3023	1,400	3GBL	0.244	58‡	3.7	0.51	4.3	6.1	6.1
3023	1,400	3GBR	0.264	56§	2.5	0.53	3.5	6.5	7.4
120.01	1,793	001P3	0.447	33.9	4.0	0.58	4.4	4.2	6.7
3024	1,825	4GBL	0.462	35	5.5	0.54	4.5	5.0	6.0
3024	1,825	4GBR	0.464	35	3.0	0.54	4.4	5.0	6.6
120.02	2,500	002P3	0.841	17.1	2.1	0.64	4.3	3.3	3.1
121.01	2,500	101GB	0.842	17.8	1.8	0.80	3.9	4.1	3.7
120.03	2,900	003P3	1.096	12.8	1.7	0.84	4.0	3.5	2.6
121.02	2,900	102GB	1.097	12.7	1.8	0.79	4.4	3.4	3.6
120.04	3,250	004P3	1.330	11.0	1.3	0.87	4.6	3.0	4.6

* Peak pressure at 0.110 sec, initial rise 94 psi.
† Peak pressure at 0.268 sec, precursor pressure 14.5 psi.
‡ Peak pressure at 0.292 sec, precursor pressure 19.5 psi.
§ Peak pressure at 0.286 sec.
¶ Not readable.

At 114.15 a definite precursor type wave form was measured, while at 115.23 the shape was essentially ideal. A satisfactory record at 115.22 was not obtained.

A look at Figure 2.1 shows that Station 3023 was almost in line with the pipes extending from the cab. Even though it was quite some distance from them, it was necessary to consider the possibility that the wave forms were caused by a jet down the pipes. Fireball pictures, however, show no evidence of any jet, so this possibility has been excluded.

There was no positive evidence about the condition of the ground at shot time. Though it had been raining almost every night, there was no definite information that it rained the night before the shot. The ground was at least damp from previous rains. It was coral sand however, which drains quite well. Thus even though the exact state of affairs is not known, it is believed that in Nevada the effects would have been more pronounced.

3.3 DYNAMIC PRESSURES

The dynamic pressure records were consistent with the overpressure records showing the precursor wave form only at Station 3023. The data points are plotted in Figure 3.3 and compared to the curves for 1.6 and 2 times the free-air values for 40 kt. The measured values of q at the 1,793-, 2,500-, and 2,900-foot stations have been corrected according to wind-tunnel tests of the pitot gage. The value measured at the 1,400-foot station, showing the precursor, has not been corrected at all. Although the pitot gage has not been calibrated in a flow of as

TABLE 3.2 DYNAMIC PRESSURE RESULTS

Station	Ground Range	Gage	Arrival Time	Peak Dynamic Pressure	Dynamic Pressure Duration	Dynamic Pressure Impulse
	ft		sec	psi	sec	psi-sec
3022	920	2q3	0.104	235	0.12	11.2
3023	1,368	3q3	0.244	180*	0.78	7.7
120.01	1,795	001q3	0.446	22.8	0.23	2.3
120.02	2,500	002q3	0.840	6.6	0.67	1.0
120.03	2,900	003q3	1.096	4.0	0.9	0.84

* Peak pressure at 0.256 sec, precursor pressure 140 psi.

high a Mach number as that at Station 3021 (920 feet), a correction based on the formation of a bow wave at the nose of the pitot tube has been applied. This correction is believed valid because high-speed photography on similar shapes shows that the reflected shock off the nose goes over into the bow wave and is well established before the incident shock reaches the static openings. This correction converts the measured differential pressure of 360 psi to a dynamic pressure of 235 psi, in good agreement with that of 244 psi calculated from the measured overpressure.

No correction to the precursor q has been made since neither the Mach number nor the contribution of dust is known. An ideal shock of 55 psi has a Mach number of about 1, if this Mach number is used to correct the measured differential pressure of 180 psi, it would only reduce it to about 140 psi at the lowest. This is still much higher than the 96-psi q associated with a 84-psi shock or the ideal (2w) 80-psi q for this distance.

3.4 IMPULSES

Both the overpressure and dynamic pressure impulses are plotted in Figure 3.4 where they are compared to the free-air values. The only comment than can be made is that the data show a wide scatter.

TABLE 3.3 OVERPRESSURE RESULTS SCALED TO 1 KT, SEA LEVEL

Station	Ground Range	Gage	Arrival Time	Peak Positive Pressure	Peak Negative Pressure	Positive Pressure Duration	Negative Pressure Duration	Positive Pressure Impulse	Negative Pressure Impulse
	ft		sec	psi	psi	sec	sec	psi-sec	psi-sec
3021	202	1GBL	0.0149	442	*	*	*	*	*
3021	202	1GBR	0.0149	372	*	*	*	*	*
3021	202	1GBR-RF	0.0149	332	*	*	*	*	*
3022	270	2GBL	0.0309	156	†	0.14	†	3.5	†
3022	270	2GBR	0.0303	133	*	*	*	*	*
3023	401	3P3	0.0725	84	4.3	0.13	0.13	1.4	2.3
3023	410	3GBL	0.0725	58	3.7	0.15	0.13	1.8	1.8
3023	410	3GBR	0.0784	56	2.5	0.16	0.10	1.9	2.2
120.01	525	001P3	0.133	34	4.0	0.17	0.13	1.3	2.0
3024	535	4GBL	0.137	35	5.5	0.16	0.13	1.5	1.8
3024	535	4GBR	0.138	35	3.0	0.16	0.13	1.5	2.0
120.02	732	002P3	0.250	17.2	2.1	0.19	0.13	1.0	0.9
121.01	732	101GB	0.250	17.9	1.8	0.23	0.12	1.2	1.1
120.03	850	003P3	0.326	12.9	1.7	0.25	0.12	1.0	0.8
121.02	850	102GB	0.326	12.8	1.8	0.23	0.13	1.0	1.1
120.04	952	004P3	0.395	11.1	1.3	0.25	0.14	0.9	1.4

* Record bad.
† Not readable.

SECRET

TABLE 3.4 DYNAMIC PRESSURE RESULTS SCALED TO 1 KT, SEA LEVEL

Station	Ground Range	Gage	Arrival Time	Peak Dynamic Pressure	Dynamic Pressure Duration	Dynamic Pressure Impulse
	ft		sec	psi	sec	psi-sec
3022	202	2q3	0.0309	236	0.036	3.3
3023	401	3q3	0.0725	181	0.23	2.3
120.01	526	001q3	0.132	22.9	0.068	0.7
120.02	732	002q3	0.250	6.6	0.20	0.28
120.03	850	003q3	0.326	4.0	0.27	0.25

TABLE 3.5 SCALING FACTORS AND AMBIENT CONDITIONS FOR SHOT LACROSSE

Ambient Pressure, P_0: 1008.5 mb
Ambient Temperature, T_0: 300 deg K
Relative Humidity: 84 percent
Winds: 16 knots from 080 degrees
Visibility: Greater than 10 miles
Tide Level: 2.2 feet above mean low water springs

Ground Zero: The device was fired 17 feet above the datum plane in a cab placed on a man-made island. The man-made island and Yvonne itself are about 10 feet above the datum plane. The device was 7 feet above the floor of the cab. The reef on which the man-made island was placed was 1 foot below the datum plane.

Function	Scaling Factor
Distance	$\left(\frac{P_0}{40 \times 14.7}\right)^{1/3} = 0.293$
Pressure	$\frac{14.7}{P_0} = 1.005$
Time	$\left(\frac{T_0}{293}\right)^{1/2} \left(\frac{P_0}{40 \times 14.7}\right)^{1/3} = 0.297$
Impulse	$\left(\frac{T_0}{293}\right)^{1/2} \left(\frac{1}{40}\right)^{1/3} \left(\frac{14.7}{P_0}\right)^{2/3} = 0.298$

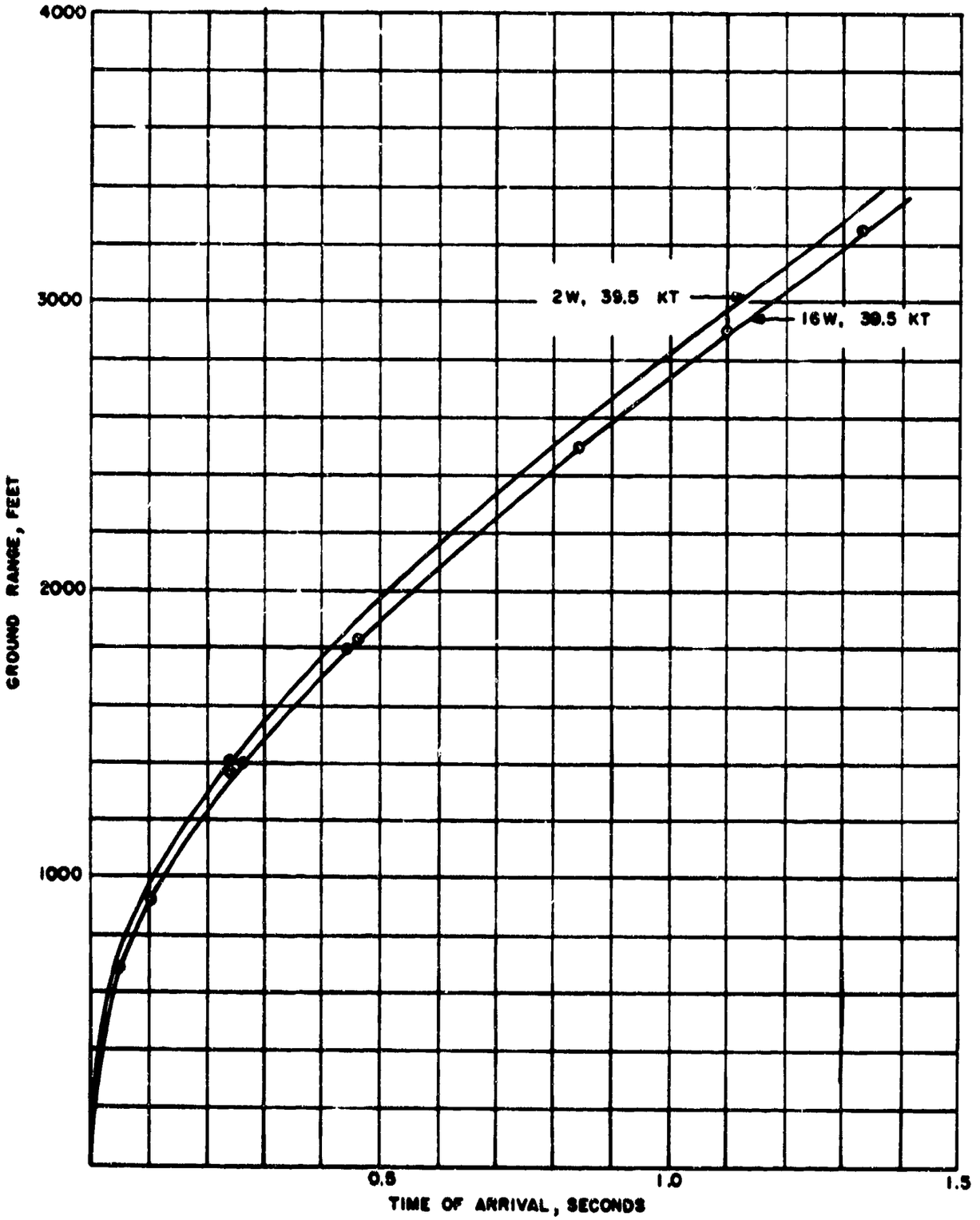

Figure 3.1 Arrival time versus ground range.

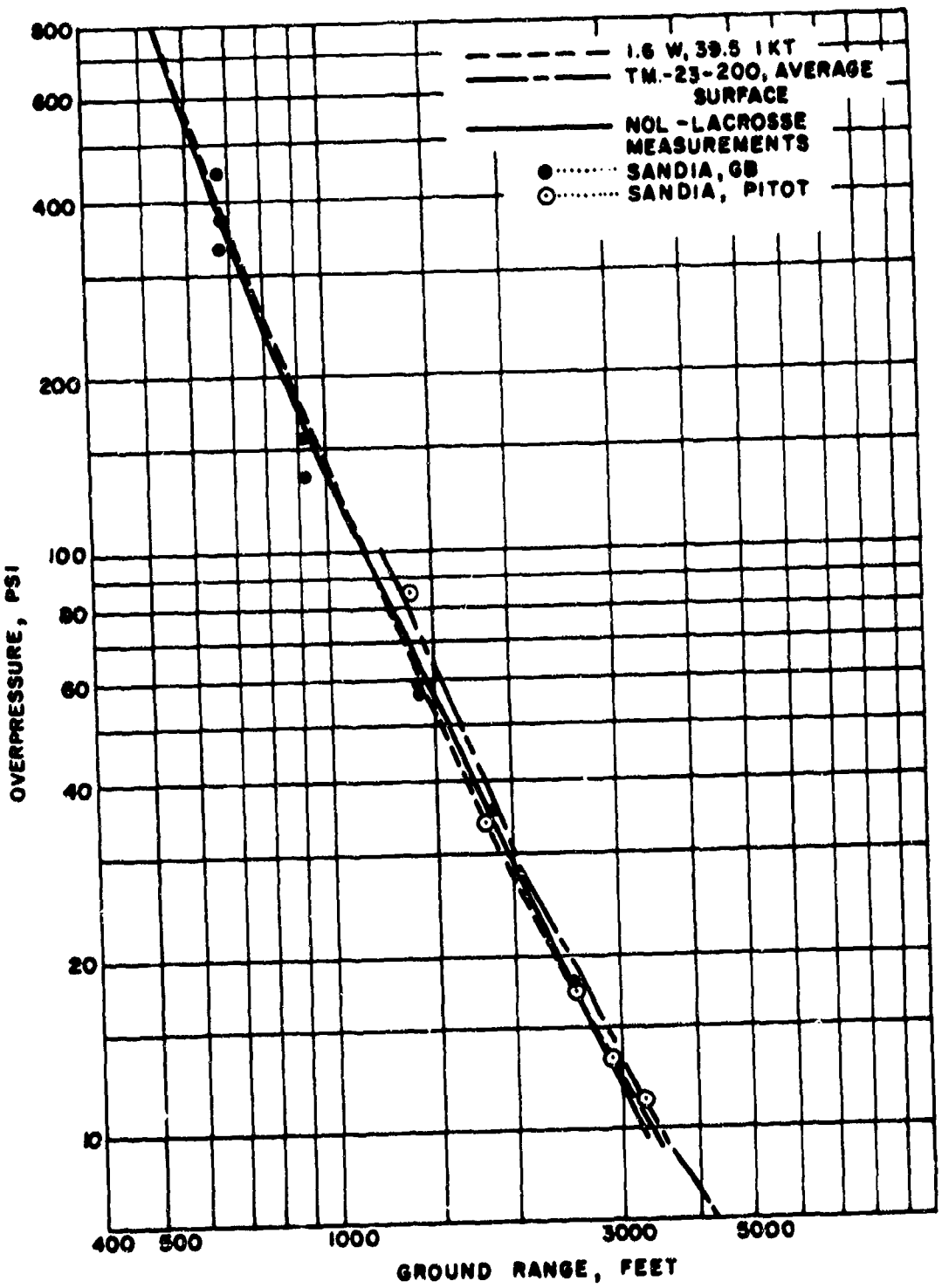

Figure 3.2 Overpressure versus ground range.

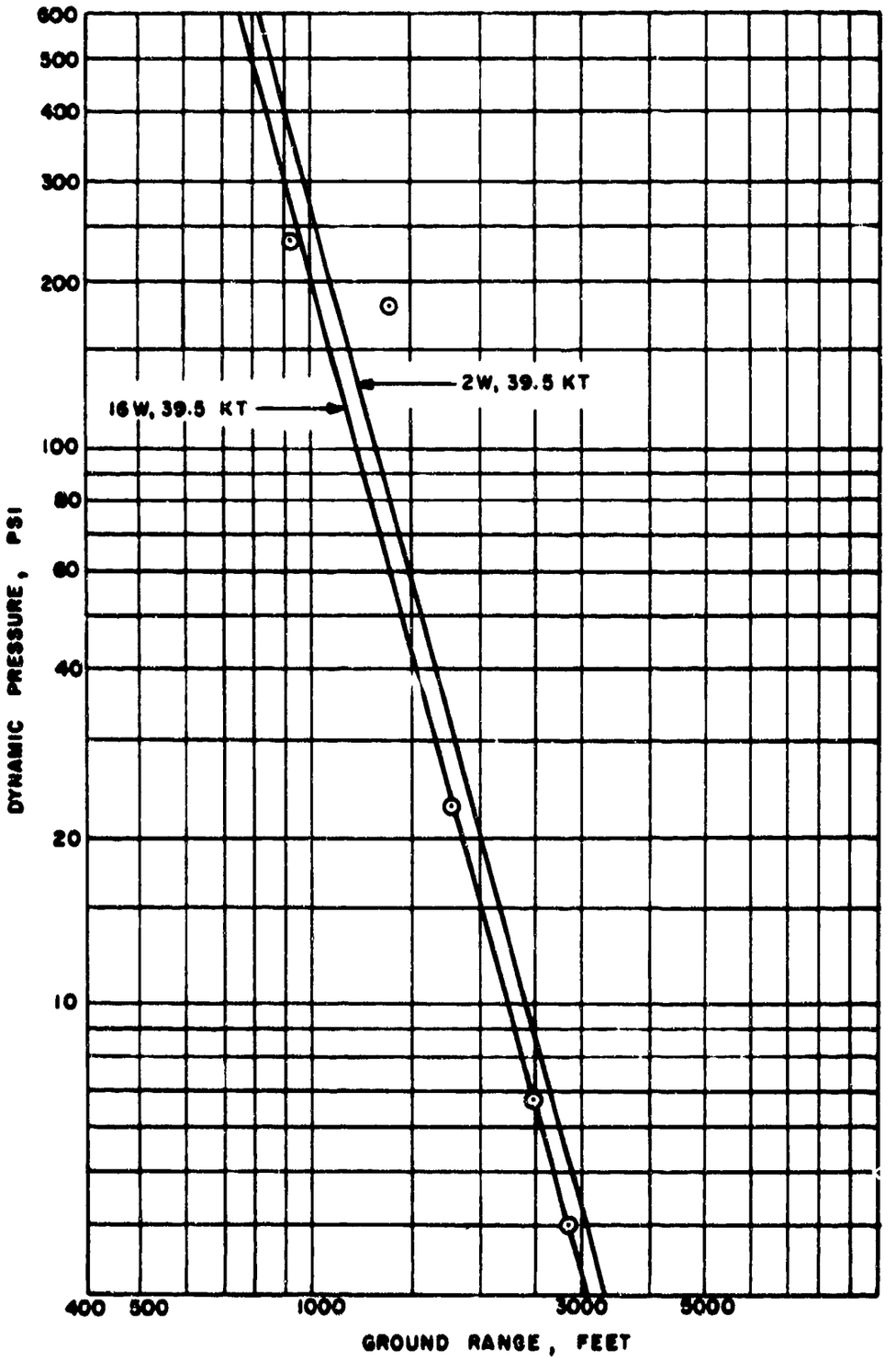

Figure 3.3 Dynamic pressure versus ground range.

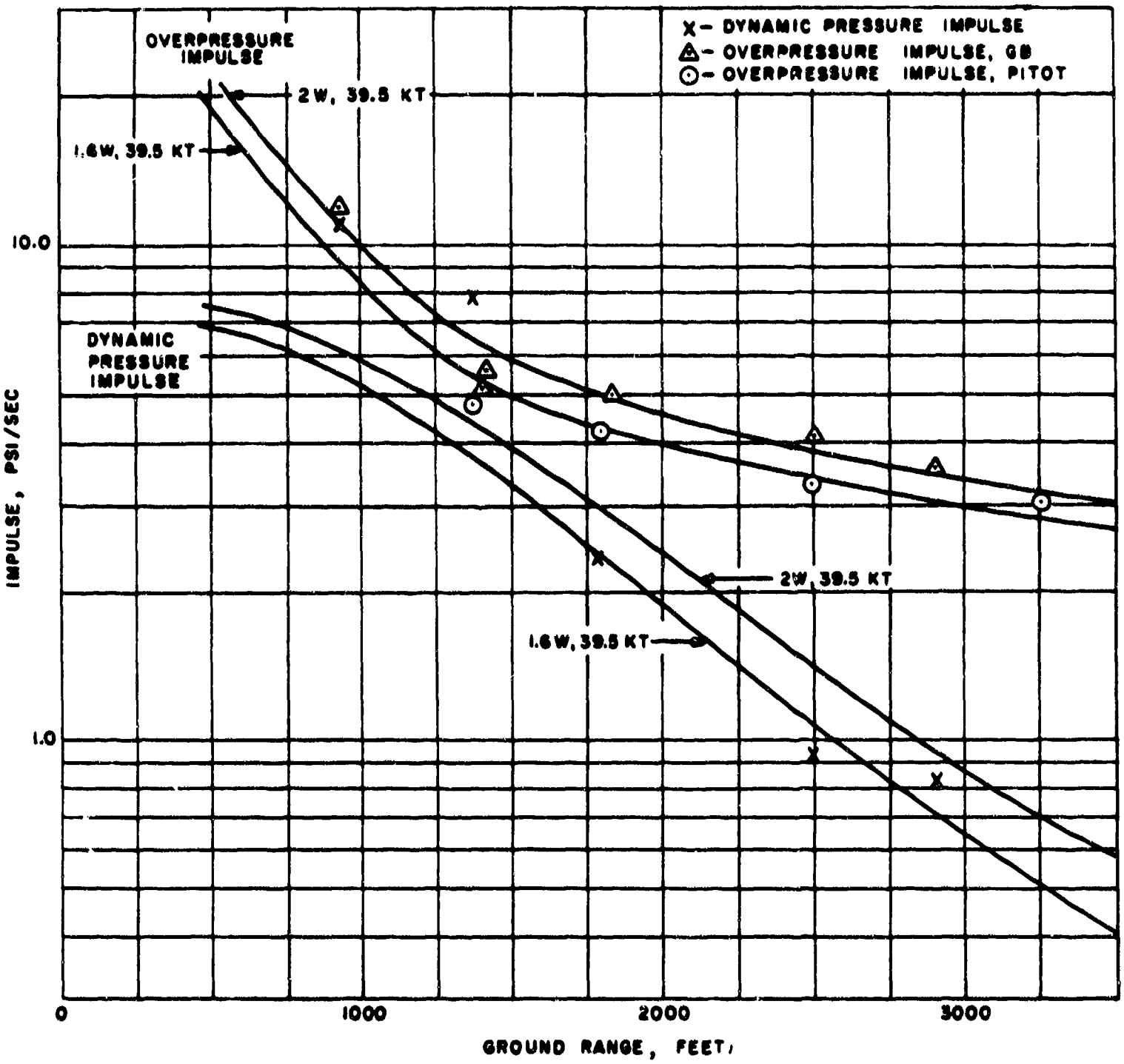

Figure 3.4 Impulse versus ground range.

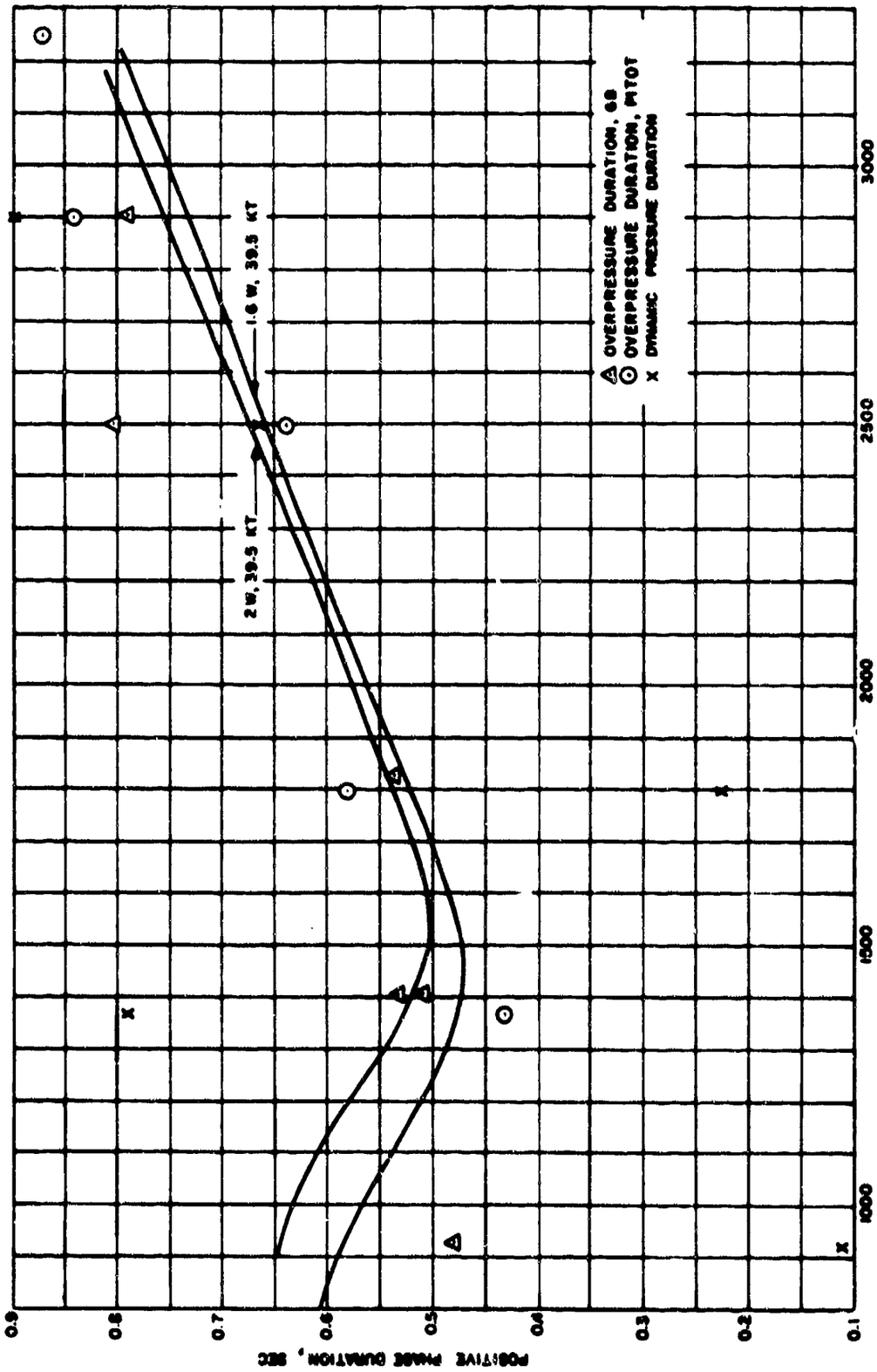

Figure 3.5 Duration versus ground range.

SECRET

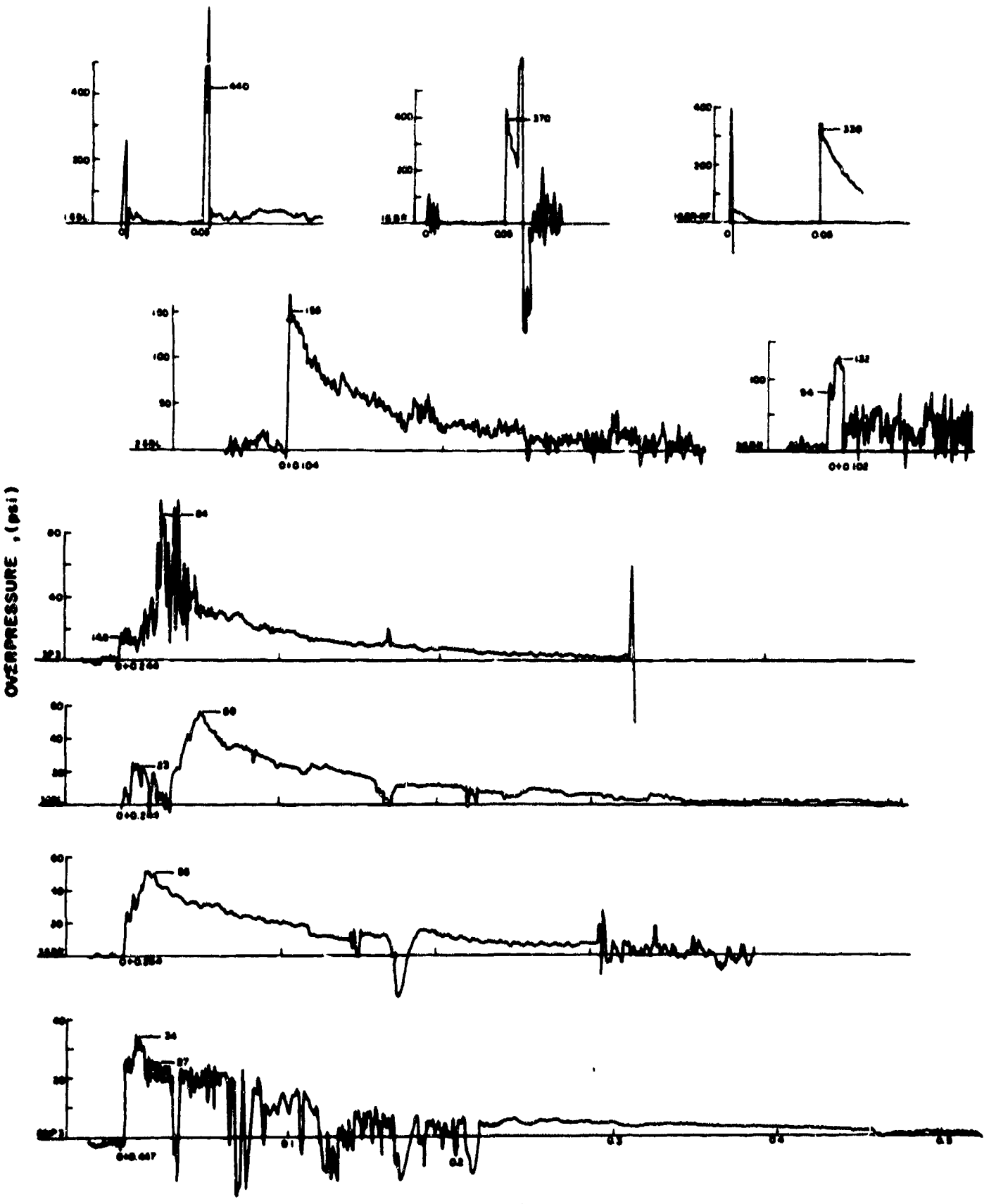

Figure 3.6 Overpressure versus time, showing shock-wave arrival time, in seconds, and history after shock arrival.

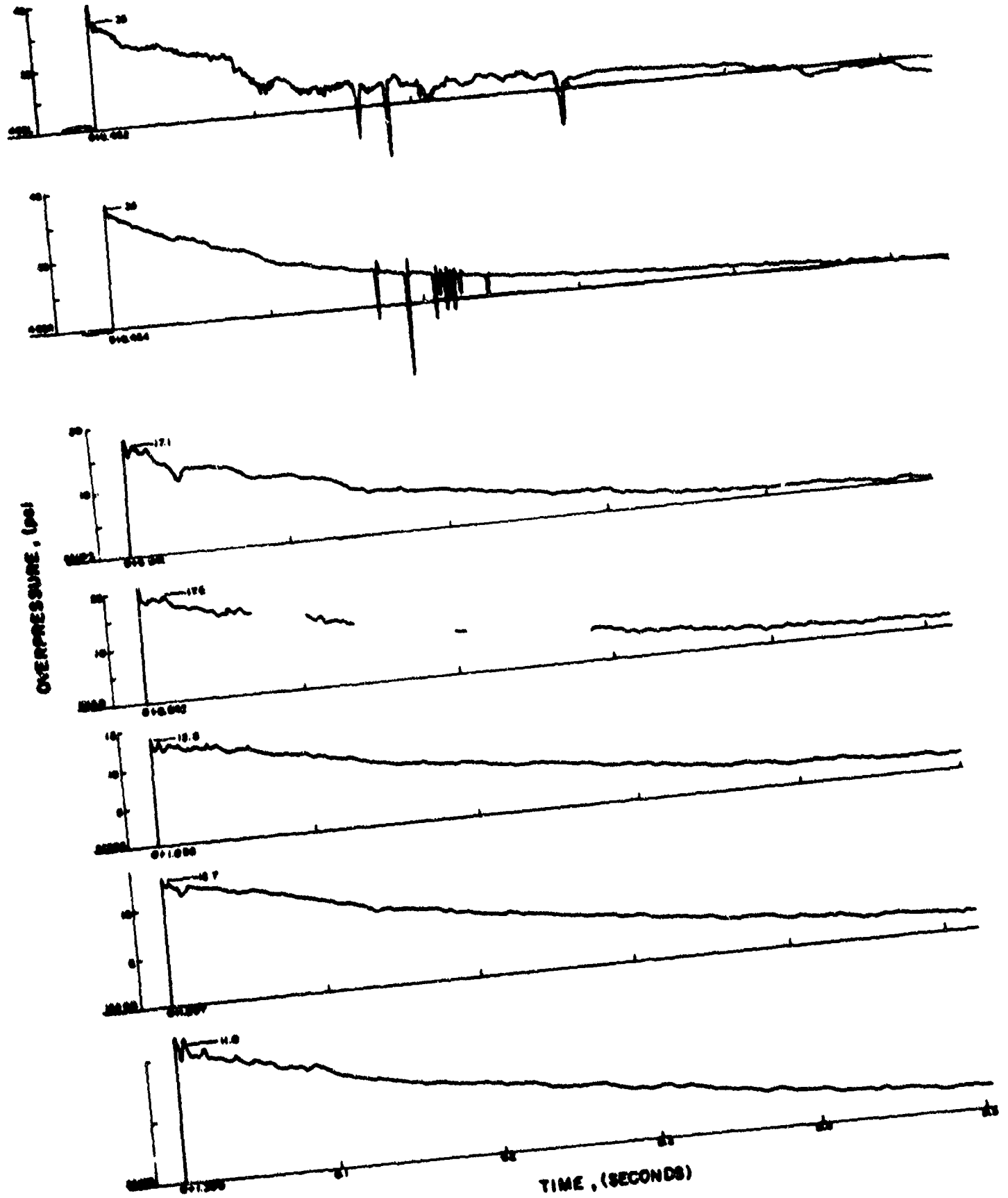

Figure 3.6 Continued.

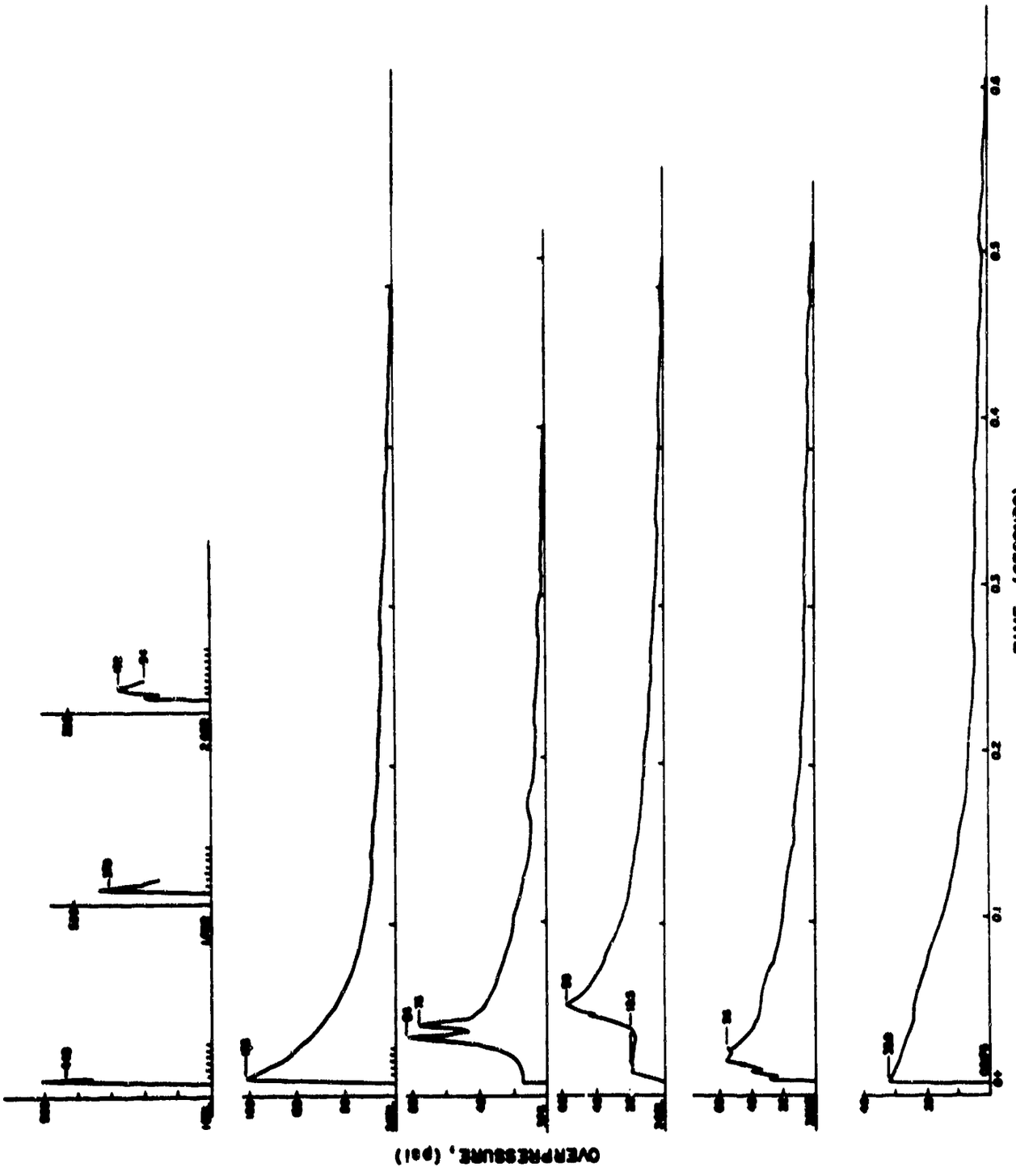

Figure 3.7 Smoothed overpressure versus time records.

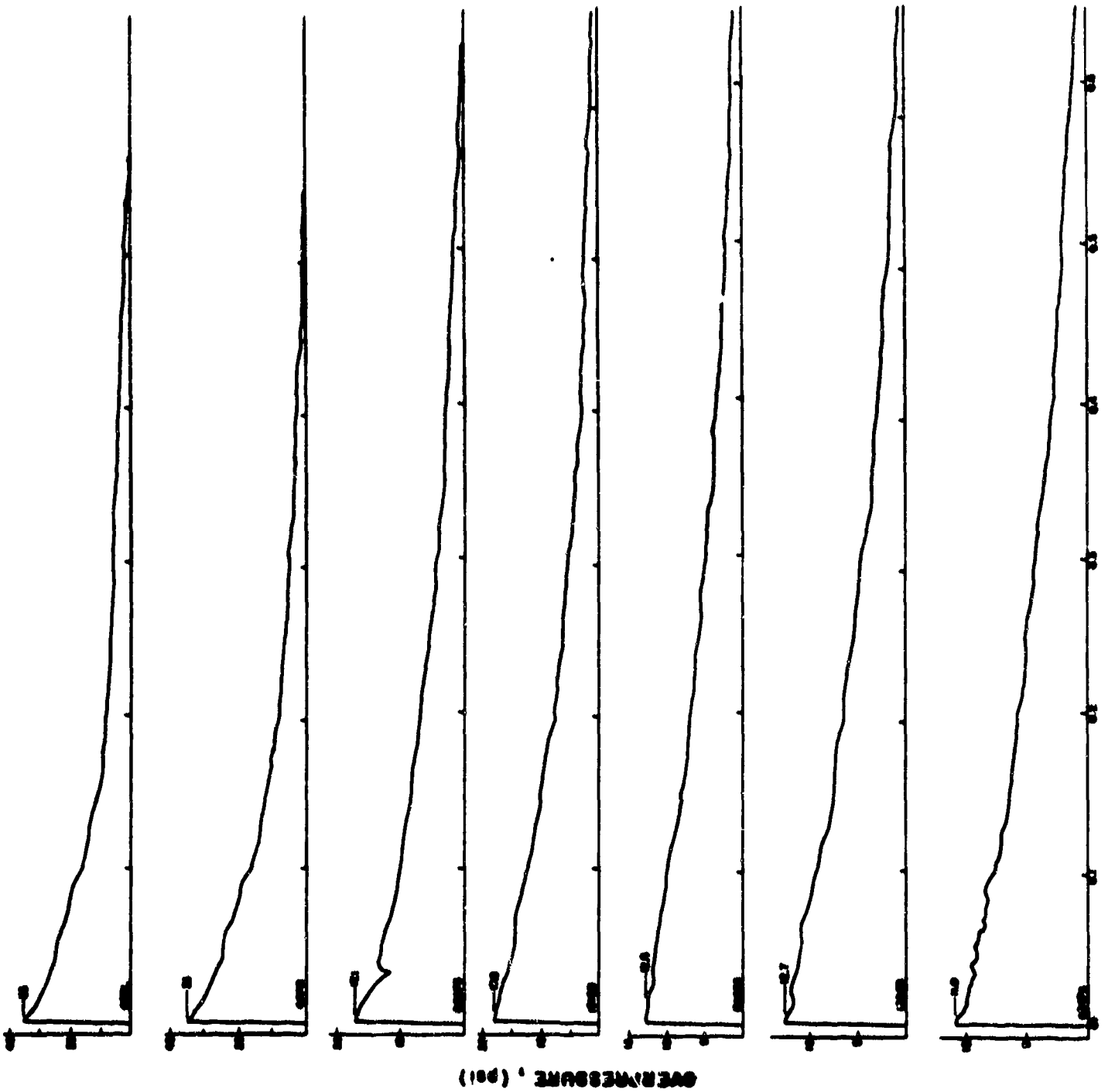

Figure 3.7 Continued.

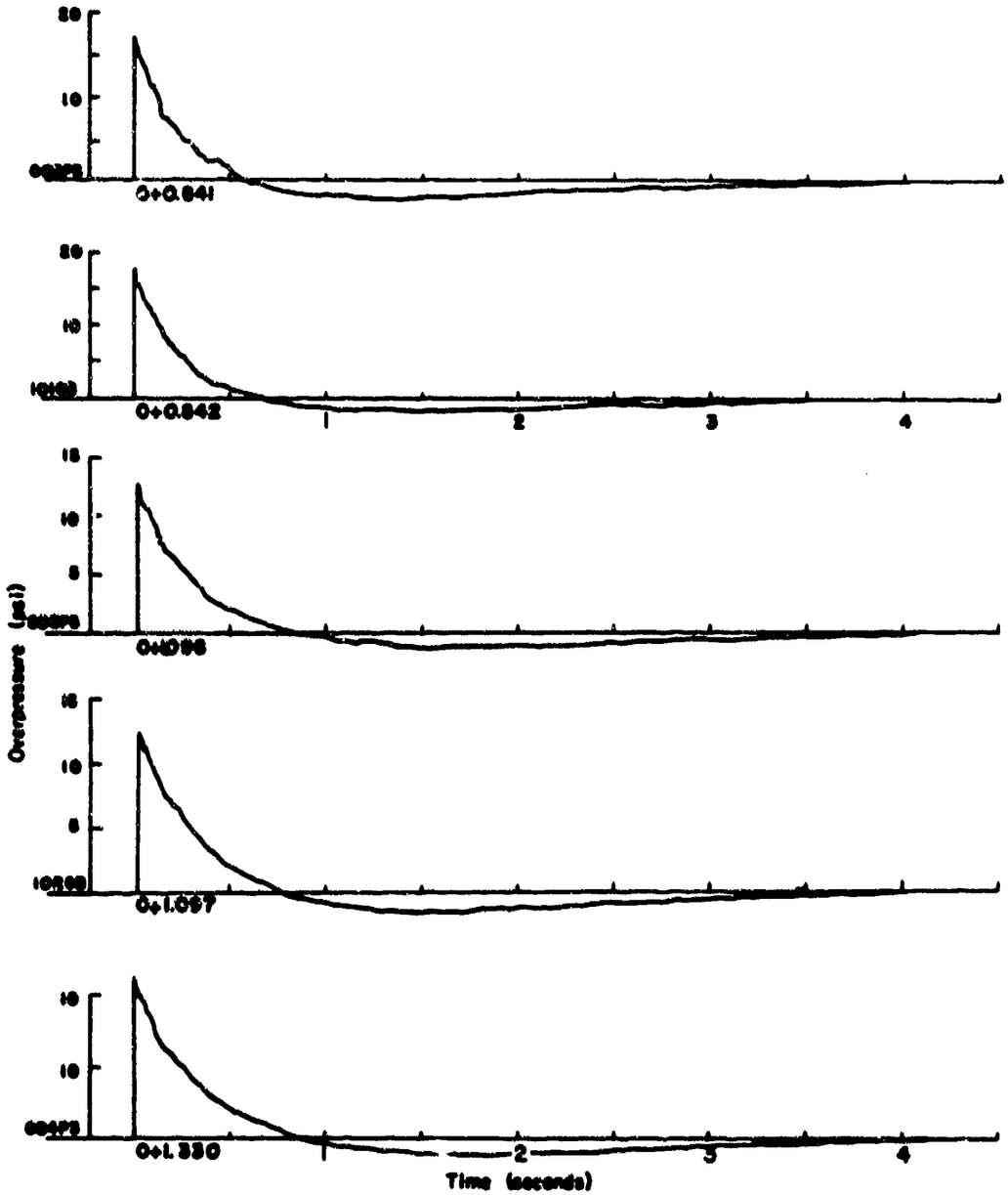

Figure 3.8 Overpressure versus time, showing shock-wave arrival time, in seconds, and history after shock arrival.

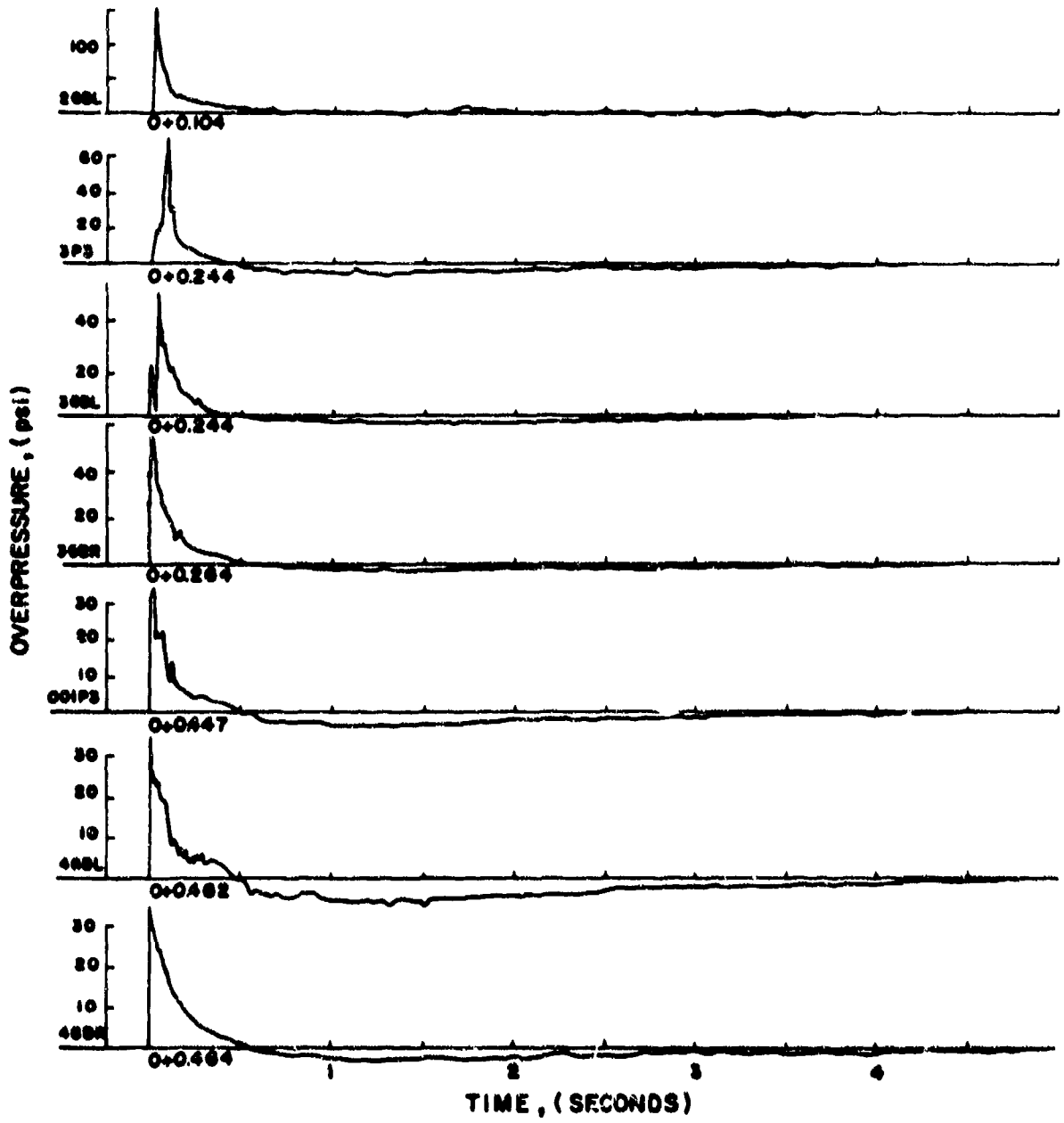

Figure 3.8 Continued.

SECRET

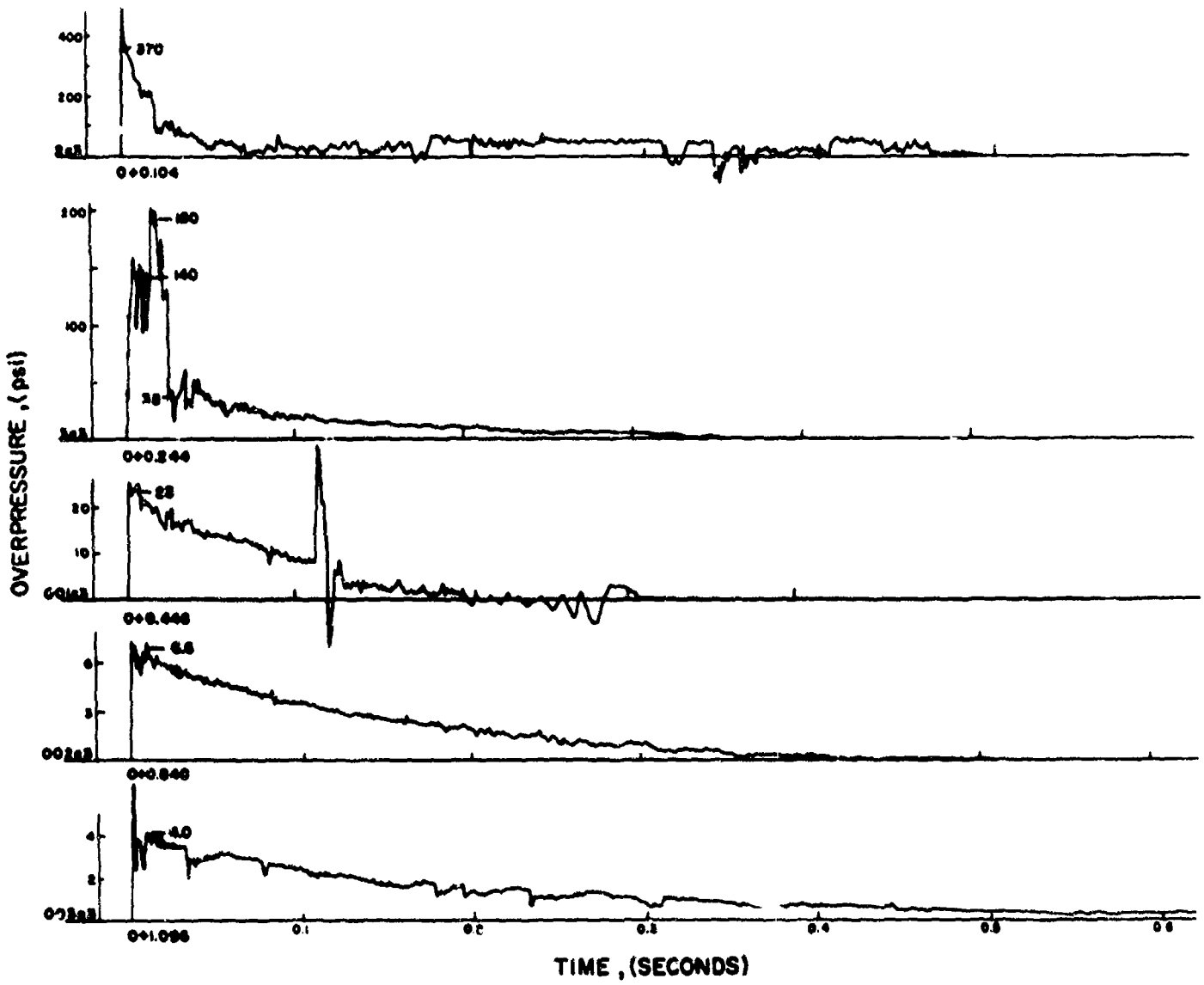

Figure 3.9 Dynamic pressure versus time records.

SECRET

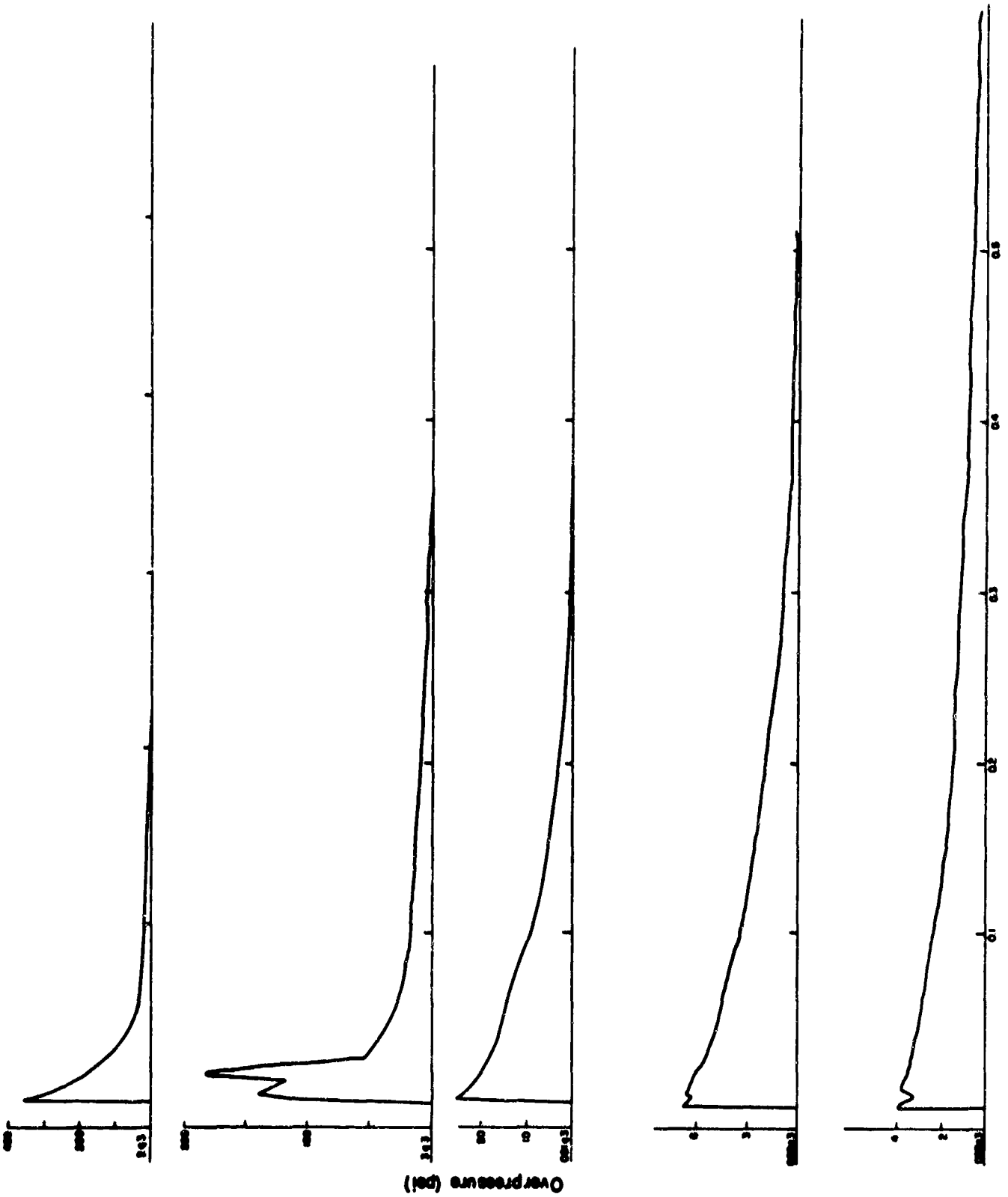

Figure 3.10 Smoothed dynamic pressure versus time records.

3.5 DURATIONS

The positive phase durations for the overpressure and the dynamic pressure are plotted in Figure 3.5. Again, about all that can be noted is the wide scatter. In both of the above cases the scatter is probably due to the same cause which is believed to be instrumental rather than a blast phenomenon.

3.6 GENERAL

The curves for $Q_{i_{ps}}$ with the $\sin\alpha$ in Figure 1.3 were used to predict that a precursor for Shot Lacrosse should be expected. The actual observed occurrence of the precursor in agreement with the prediction may have been somewhat fortuitous since the thermal measurements indicated considerably less thermal yield than the 10 kt used for the prediction. It is somewhat difficult to interpret the thermal measurements (Reference 18). In the direction of the large mass of pipe and concrete on one side of the burst, the thermal measurements indicated between 3 and 4 kt, while in the other direction, which was relatively free of such obstructions, somewhat over 5 kt was measured. Pressure stations were at an angle in between these two measurements and at much closer distances. Measurements indicated that the thermal energies at close distances would be greater than those predicted from the measurements at large distances with an assumption that the thermal energy was inversely proportional to the distance squared; however, no close measurements were available for this shot and such corrections were not made to the other shots which were shown in Figure 1.3.

The use of a thermal yield of 5 kt gives the curve marked L in Figure 1.3, and it is obvious that one would not predict a precursor from this curve. No further comments can be made to explain the occurrence of the precursor with this curve except to comment that perhaps the nature of Shot Lacrosse was exceptional and that actual thermal received at the close ranges was exceptionally high compared to the distant measurements; i.e., exceptionally high even compared to this tendency which has been observed on other shots.

In addition to the measurements reported here, the Ballistic Research Laboratories (Reference 17) found that a precursor was formed on Shot Zuni, a surface burst of approximately 3 Mt. It was observed on two blast lines 180 degrees apart on one line extending to at least 24 psi. The meager data there indicated a more extensive precursor for Shot Zuni than for Shot Lacrosse. Since Castle 6 had little, if any, precursor effect, it would appear that other factors such as surface conditions perhaps are more important than yield in determining that precursors will form on surface bursts.

Chapter 4
CONCLUSIONS and RECOMMENDATIONS

4.1 CONCLUSIONS

The measured overpressures and the dynamic pressures were in good agreement with previous measurements (References 3 and 5); that is, they corresponded to the free-air values for 1.6 times the yield of 39.5 kt. A precursor of limited extent was formed that had typical distorted wave forms and for which the dynamic pressure was abnormally high. The evidence from Castle 6, Shot Lacrosse, and Shot Zuni indicates that for surface bursts the severity of the precursor for surface bursts can depend appreciably on the ground surface condition, as well as the factor of shock arrival time and thermal radiation incident normal to the ground. Any attempt to predict in detail requires more information not only for the PPG terrain but for other types of soil surfaces.

4.2 RECOMMENDATIONS

Information about precursor formation on surface bursts is necessary in order to decide how best to fuze and employ weapons as well as to evaluate their damage capabilities. In order to obtain this information about surfaces of practical importance an experiment over these surfaces or at least over a dry desert-type surface should be performed so that there will be two points to interpolate between instead of just one point from which to extrapolate.

REFERENCES

1. "Blast and Shot Measurement II"; Project 1.2b, Operation Buster-Jangle, WT-367, 1951; NSWU 471, Field Command, AFSWP, Sandia Base, Albuquerque, New Mexico; Secret Restricted Data.

2. G.W. Rollosson; "Air Shock Pressure-Time Versus Distance"; Project 6.1, Operation Ivy, WT-602, April 1953; Sandia Corporation, Albuquerque, New Mexico; Secret Restricted Data.

3. C.D. Broyles and M.L. Merritt; "Ground Level Pressures from Surface Bursts"; Project 1.2a, Operation Castle, WT-904, October 1957; Sandia Corporation, Albuquerque, New Mexico; Secret Restricted Data.

4. Maynard Cowan, Jr.; "Shock Winds, and Changes in Air Temperature Resulting from Large Atomic Bursts Near the Earth's Surface"; Project 6.3, Operation Ivy, WT-603; May 1953; Sandia Corporation, Albuquerque, New Mexico; Secret Restricted Data.

5. C.D. Broyles and M.L. Merritt; "Dynamic Pressure Measurements"; Project 1.3, Operation Castle, WT-906, January 1958; Sandia Corporation, Albuquerque, New Mexico; Secret Formerly Restricted Data.

6. P. Hanlon; "Blast Pressures and Shock Phenomena Measurements by Photography"; Projects 1.1a, 1.1b and 1.1d, Operation Castle, WT-902, September 1955; U.S. Naval Ordnance Laboratory, White Oak, Maryland; Secret Restricted Data.

7. F.H. Shelton; "The Precursor, Its Formation, Prediction, and Effects"; SC-2850(TR), July 27, 1953.

8. H. Scoville, et al; Final Summary Report; Operation Tumbler-Snapper, WT-514, May 1953; AFSWP, Washington, D.C.; Secret Restricted Data.

9. F.M. Sauer; "The Preshock Sound Velocity Field Over Inorganic and Organic Surfaces"; AFSWP-420, December 1954.

10. Summary Report of the Technical Director, Programs 1-9; Operation Teapot, WT-1153, 1955; Secret Restricted Data.

11. A.F. Robertson; "Final Report on the Effects of Thermal Radiation on Materials"; National Bureau of Standards, AFSWP-281, November 1, 1953.

12. W.E. Morris, et al; "Air Blast Measurements"; Projects 1.1a and 1.2, Operation Upshot-Knothole, WT-710, August 1955; U.S. Naval Ordnance Laboratory, White Oak, Silver Spring, Maryland; Secret Restricted Data.

13. L.M. Swift and D.C. Sachs; "Air Pressure and Ground Shock Measurements"; Project 1.1b, Operation Upshot-Knothole, WT-711, January 1955; Stanford Research Institute, Menlo Park, California; Secret Restricted Data.

14. L.B. Streets; "Basic Characteristics of Thermal Radiation from an Atomic Detonation"; AFSWP-503, November 1953.

15. R.H. Thompson; "Instrumentation for Projects 1.2a, 1.3 and 1.7"; Projects 1.2a, 1.3 and 1.7, Operation Castle, WT-907, 1954; Sandia Corporation, Albuquerque, New Mexico; Confidential.

16. D.C. Sachs, L.M. Swift and F.M. Sauer; "Airblast Overpressure and Dynamic Pressure Over Various Surfaces"; Project 1.10, Operation Teapot, WT-1109, September 1957; Stanford Research Institute, Menlo Park, California; Confidential Formerly Restricted Data.

17. C.N. Kingery, C.H. Hoover and J.H. Keefer; "Basic Surface Blast Measurements"; Operation Redwing, WT-1301 (to be published).

18. R.W. Hillendahl; "Basic Thermal Radiation Measurements from Ground Stations"; Project 8.1a, Operation Redwing, WT-1338, May 1959; U.S. Naval Radiological Defense Laboratory, San Francisco 24, California; Secret Restricted Data.

Appendix
THERMAL FLUX from a SURFACE BURST

Photometric relations (Reference 19, page 140) can be useful in the calculation of the radiation flux into the ground from a hemispherical source at the surface if the source is a perfect or uniformly diffusing surface. By this is meant a surface that appears equally bright from any direction. This is not always true for a fireball but is probably a good approximation during the early part of the radiation at least. It is a photometric principle (Reference 19, page 145) that a uniformly diffusing surface is equivalent to any other such surface that intercepts the same solid angle as far as calculating the radiation flux is concerned. Thus a hemisphere can be replaced by a semi disk (Figure A.1) for calculation of the flux at a point P. The flux from the disk, m, through a surface at P parallel to the plane of the hemisphere base is given by (Reference 19, page 143):

$$F = B\left\{\tan^{-1}\frac{m}{f} - \frac{mf}{m^2+f^2}\right\} \qquad (A.1)$$

or using the geometrical relation between m, f, and r, d:

$$F = B\left\{\sin^{-1}\frac{r}{d} - \left(\frac{r}{d}\right)^2\left[\left(\frac{d}{r}\right)^2 - 1\right]^{1/2}\right\}$$

Here πB is the flux per unit area of the emitter surface. Replacing B with the total thermal output, I, of the hemisphere,

$$F = \frac{I}{2(\pi r)^2}\left\{\sin^{-1}\frac{r}{d} - \left(\frac{r}{d}\right)^2\left[\left(\frac{d}{r}\right)^2 - 1\right]^{1/2}\right\} \qquad (A.2)$$

where $I = 2\pi r^2(\pi B)$. The last equation can be rewritten in terms of the flux, $F_p = I/4\pi d^2$, from a point source through a surface normal to a radius, thus:

$$F = \frac{I}{4\pi d^2}\left(\frac{d}{r}\right)^2\frac{2}{\pi}\left\{\sin^{-1}\frac{r}{d} - \left(\frac{r}{d}\right)^2\left[\left(\frac{d}{r}\right)^2 - 1\right]^{1/2}\right\}$$

$$= F_p\,\phi$$

The factor ϕ varies from 1.0 for a point at the surface of the hemisphere to zero at infinity. Figure A.2 is a plot of ϕ versus r/d.

To use this relation correctly to calculate the normal component of radiation delivered before shock arrival would require an integration:

$$\int_0^t F\,dt = \int_0^t \frac{I(t)}{4\pi d^2}\,\phi\left(\frac{r}{d}\right)dt \qquad (A.3)$$

where $\phi(r/d)$ is also a function of time, since r, the fireball radius, is increasing during the radiation. Such a calculation could be made numerically since the empirical curves of r and I versus t are known. This has, however, not yet been done. For the purpose of this report, the shape of the radiation flux versus time is such that it seemed reasonable to assume an effective r/d for each time point chosen for calculation. This is because most of the growth of the fireball takes place during the period when only a small part of the energy is being radiated.

Use of this method along with the point source calculations is best illustrated by an example. Greenhouse Dog (GD) was chosen for the example since it combines both methods. The various quantities used are tabulated in Table A.1 and are plotted in Figure A.3. At the 1,000-, 1,500-, and 2,000-foot ranges the values of $Q_{\perp ps}$ have been calculated by both methods. In the graph the curve has been drawn nearly through the points from the ϕ function at the 1,500- and 2,000-foot ranges, because looking at the percent emission column it is seen that practically all the thermal received at these distances came after the fireball became hemispherical. At 1,000 feet the curve was drawn between the two points since an appreciable portion of the radiation was received before the fireball became hemispherical. At 500 feet the shock arrived just at thermal minimum. The radiation in the first peak was taken as 0.7 percent; since the fireball touched the ground at 0.006 second or about one-fourth of the time to minimum, well over half this amount had been radiated before the fireball had begun to distort. Therefore, this position was treated as receiving its radiation from a point source.

Although no attenuation was included in these calculations it could, of course, be included. However, for large-yield devices where the radiation source is several hundred feet in radius this is not a simple

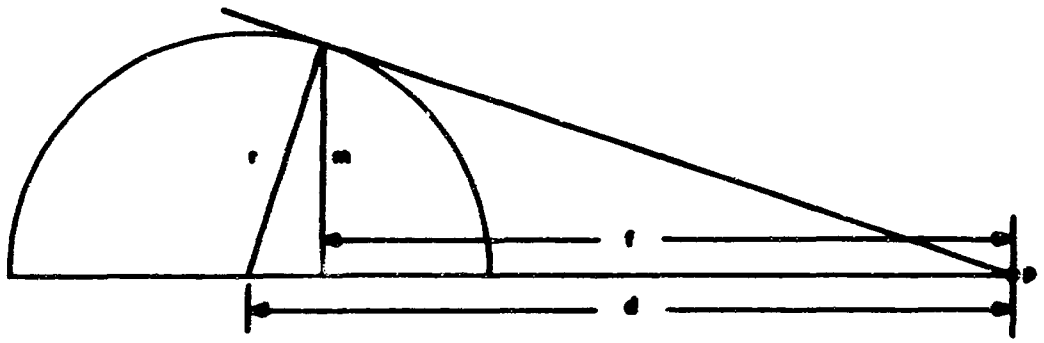

Figure A.1 Hemispherical diffusing surface and equivalent disc.

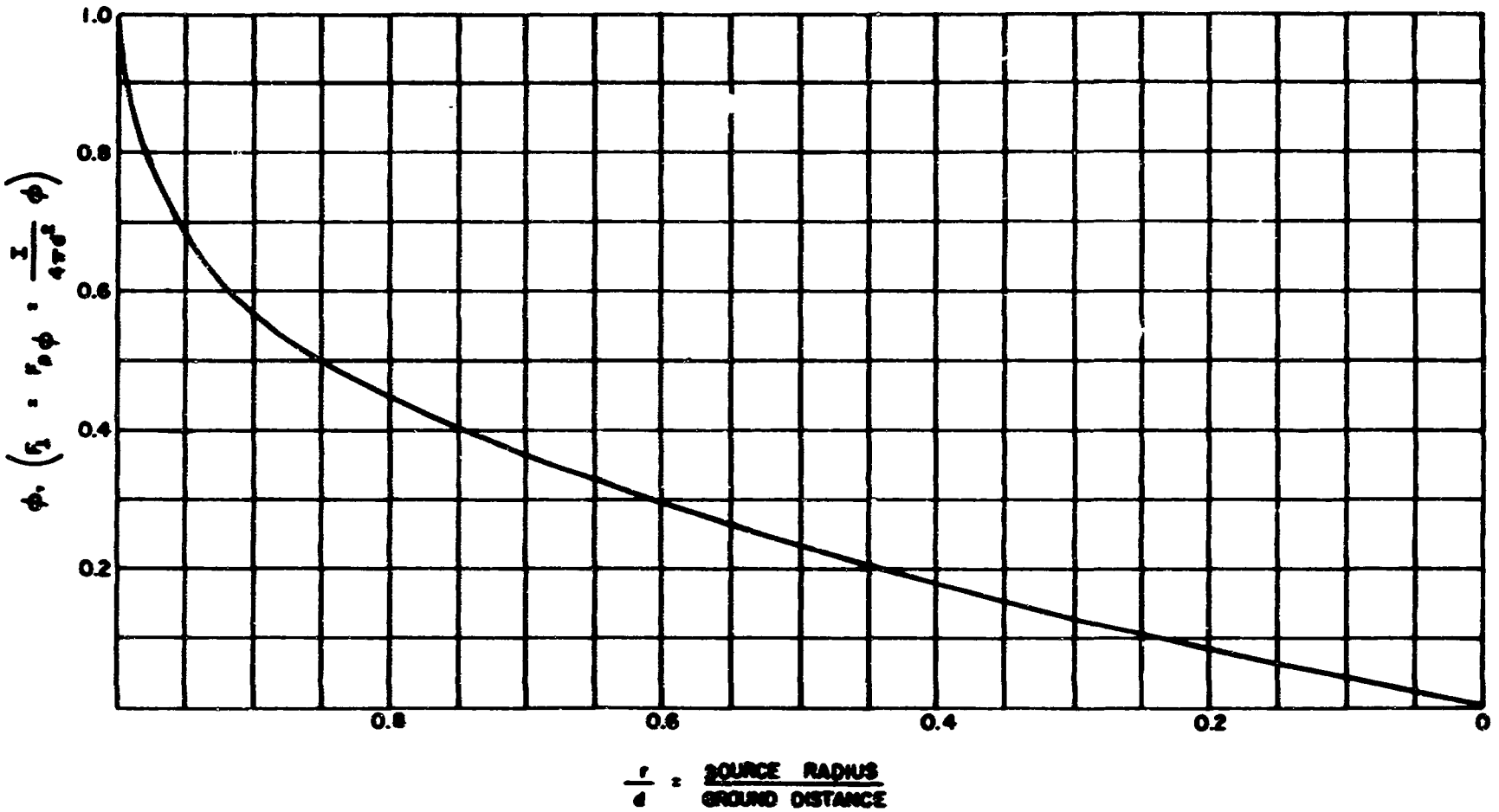

Figure A.2 Component of radiation normal to surface from a hemispherical source.

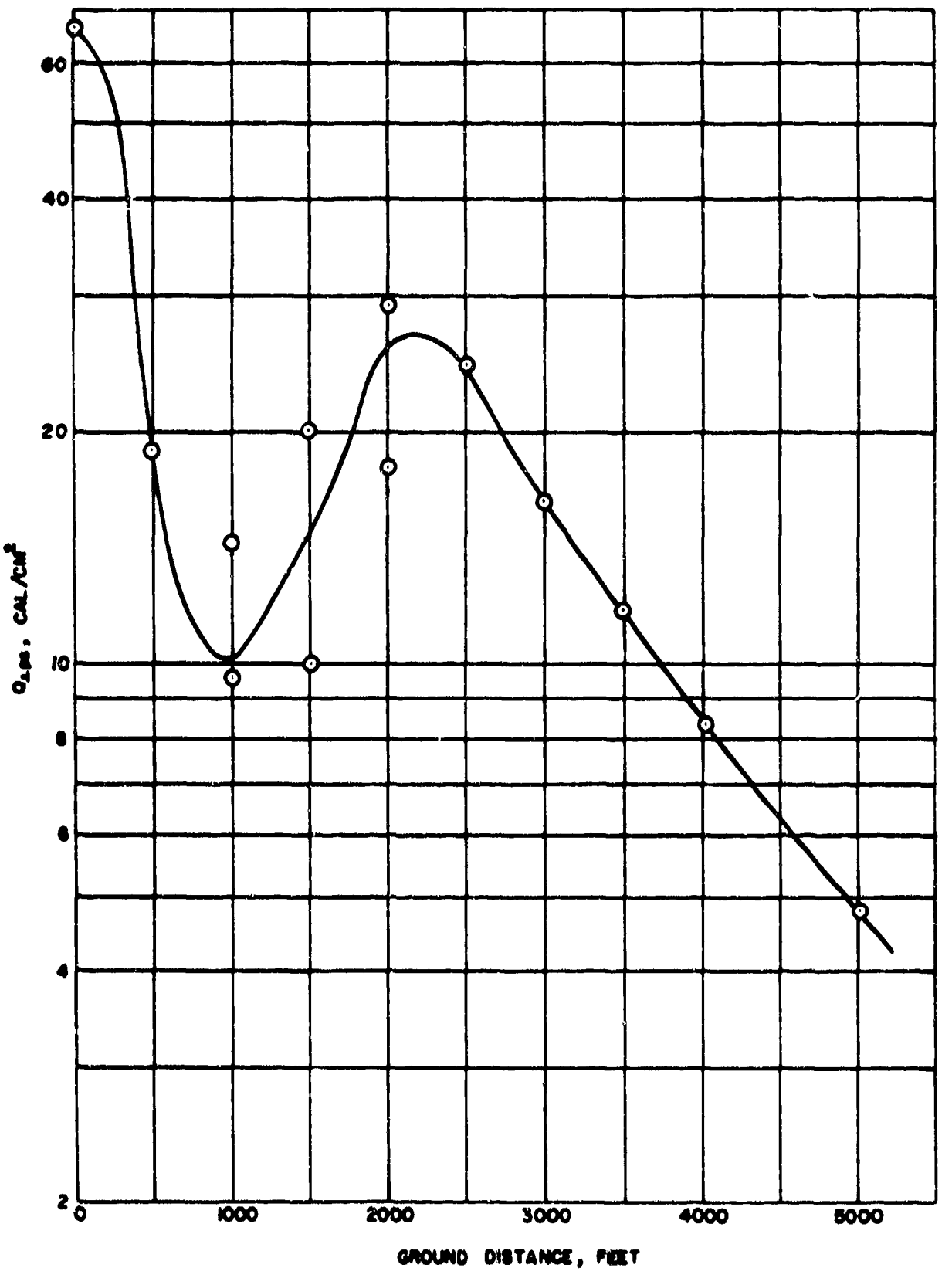

Figure A.3 Greenhouse Dog thermal radiation versus ground distance.

matter for atmospheric conditions similar to those encountered in testing at the EPG.

To summarize, details have been presented for a method of extending the calculation of preshock thermal radiation to surface bursts. It is recognized that several approximations in the calculations themselves are used. Additionally, the degree to which the assumptions about the type of source are true is uncertain and the relation of these calculated thermal values to precursor formation is not at all fully understood.

TABLE A.1 GREENHOUSE DOG PRESHOCK THERMAL RADIATION

Ground Range	Arrival Time	r/d Effective	Q_p*	Preshock Thermal	Cos α	ϕ	$Q_{\perp ps}$ from cos α	$Q_{\perp ps}$ from ϕ
ft	sec		cal/cm^2	pct			cal/cm^2	cal/cm^2
0	0.006	—	16,700	0.4	1.000	—	67	—
500	0.025	—	4,310	0.7	0.626	—	19	—
1,000	0.095	0.7	1,510	2.5	0.287	0.38	9.6	14.4
1,500	0.215	0.6	680	10	0.195	0.30	12	20.0
2,000	0.383	0.5	365	33	0.148	0.24	18	29.0
2,500	0.592	0.44	246	48	—	0.20	—	24.0
3,000	0.858	0.37	171	59	—	0.16	—	16.6
3,500	1.200	0.32	125	67	—	0.14	—	11.8
4,000	1.565	0.27	96	72	—	0.12	—	8.4
5,000	2.250	0.22	62	78	—	0.10	—	4.8
6,000	2.986	0.184	42	82	—	0.08	—	2.6

*Q_p is the thermal radiation from a point source, of the rated thermal yield, through a surface normal to a radius from the source, i. e., the integral of F_p in Equation A.2.

Defense Nuclear Agency
6801 Telegraph Road
Alexandria, Virginia 22310-3398

IMTI 31 March 1994

MEMORANDUM FOR DEFENSE TECHNICAL INFORMTION CENTER
ATTENTION: FDAB

SUBJECT: Declassification of Technical Reports

Reference the following DTIC accession numbers:

AD-344933L ✓ - WT-1309 OK
AD-356274L ✓ - WT-602 OK
AD-361769L - WT-1302 S FRD

The Defense Nuclear Agency Security Office has declassified all of the referenced technical reports.

The following distribution statement applies:

Approved for public release

FOR THE DIRECTOR:

G. RUBINK
Chief, Technical Information